Journal of South American Earth Sciences 35 (2012) 10–26

Contents lists available at SciVerse ScienceDirect

Journal of South American Earth Sciences

journal homepage: www.elsevier.com/locate/jsames

A modern subtropical playa complex: Salina de Ambargasta, central Argentina

Gabriela A. Zanor [a,*], Eduardo L. Piovano [a], Daniel Ariztegui [b], Christine Vallet-Coulomb [c]

[a] Centro de Investigaciones Geoquímicas y de Procesos de la Superficie CIGES, CICTERRA, Facultad de Ciencias Exactas, Físicas y Naturales, Universidad Nacional de Córdoba, Av. Velez Sarsfield 1611, X5016GCA Córdoba, Argentina
[b] Section des Sciences de la Terre et de l'environnement, Université de Genève, Rue des Maraîchers 13, 1205 Genève, Switzerland
[c] CEREGE, UMR6635, Aix-Marseille Université, CNRS, IRD, Europôle Méditerranéen de l'Arbois, BP 80 13545 Aix-en-Provence Cedex 4, France

ARTICLE INFO

Article history:
Received 3 February 2011
Accepted 26 October 2011

Keywords:
Argentina
Playa
Sedimentary subenvironment
Mudflat
Ephemeral saline lake
Evaporite
Seasonal variability

ABSTRACT

Salina de Ambargasta is a playa located at mid latitudes in central Argentina (29 °S–64 °W). Because of its hydrological behaviour, this playa complex can be subdivided into a closed system "*sensu-stricto*" and an "open-like system" due to the presence of a seasonal outflow. Geomorphological and sedimentological features enable the separation of the Ambargasta playa into well-defined western, eastern and northern zones, where aeolian processes, groundwater supply and surface inflow, respectively, define distinctive sedimentary environments and typical processes of deposition. The following depositional settings were recognized: (1) alluvial fan; (2) sandflat; (3) springs; (4) dunes and palaeo-dune field; (5) dry mudflat; (6) capillary mudflat; (7) ephemeral saline lake (includes saline mudflat and salt pan).

The dry mudflat is present at the highest topographical zone, where the groundwater influence is less important and only intermittent ponds are present. In the capillary mudflat, evaporite sedimentation is limited to the development of efflorescence by evaporative pumping. The ephemeral saline lake, placed in the lowermost topographical region, alternates cycles of lake expansion and contraction responding to inter-annual hydrological variability as well as to seasonal variability. Lake expansion takes place during early austral summer (December–March), while continuous evaporation of brine leads to the growth of halite crystals during late summer. Sodium chloride-type brines result from both chemical fractionation as evaporation increases and salt dissolution. The isotopic compositions of surficial and underground waters ($\delta^{18}O$ and $\delta^{2}H$) indicate that lake waters become isotopically enriched during summer when evaporation plays a significant role in the playa complex.

1. Introduction

Playa settings are dynamic landforms presenting an active and interrelated set of sedimentary environments mainly controlled by the hydrological balance (Hardie et al., 1978; Handford, 1981). A playa is defined as an intracontinental basin with a negative water balance – i.e. when evaporation exceeds rainfall – for more than half of the year (Rosen, 1994). Since each playa may reflect seasonal, annual and secular changes in the environment, these variations may be recorded in the sedimentary infilling of the saline basin providing useful environmental archives of past fluctuations (Sylvestre et al., 1999; Valero-Garcés et al., 2000; Bobst et al., 2001; Grosjean et al., 2003; Fritz et al., 2004). The sedimentological and mineralogical characterisation of the present-day depositional complex and its dynamics (Last and Schweyen, 1983; Last, 1984; Renaut and Long, 1989; Smoot and Lowenstein, 1991; Warren, 1999) as well as the analyses of processes affecting the geochemical evolution of brines (Hardie and Eugster, 1970; Eugster and Jones, 1979; Spencer et al., 1985; Yan et al., 2002; Richaser et al., 2003) are crucial for a comprehensive understanding of the main processes acting in evaporative systems.

Tectonics and climate are major factors controlling the distribution and features of modern evaporite environments – i.e. playas and hypersaline lakes – around the world (e.g., Allen and Collinson, 1986; Talbot and Allen, 1996; Last and Vance, 1997; Cohen, 2003; Jones and Deocampo, 2003; Lowenstein et al., 2003). However, the number of closed systems is considerable higher at subtropical latitudes (Schreiber, 1986). In particular, in southern South America, evaporites accumulate in a wide variety of settings including the elevated plateaus of the Andean Altiplano and Puna (Abbott et al., 2003; Lowenstein et al., 2003; Moreno et al., 2007), the Pampean region (Dargám, 1994; González and Maidana, 1998; Piovano et al., 2002; 2004), and the steppe region of Patagonia in the rain shadow area east of the Andes (Brodtkorb, 1999). Studies of closed basins at

* Corresponding author. Present address: División de Ciencias de la Vida DICIVA, Campus Irapuato-Salamanca, Universidad de Guanajuato, Carretera Irapuato-Silao Km 9, C.P. 36500 Irapuato, Guanajuato, México. Tel.: +52 462 624 52 15x118; fax: +52 462 624 86 78.
E-mail addresses: gzanor@ugto.mx, gzanor@hotmail.com (G.A. Zanor).

0895-9811/$ – see front matter © 2011 Elsevier Ltd. All rights reserved.
doi:10.1016/j.jsames.2011.10.007

mid latitudes – i.e. south of the Tropic of Capricorn – in South America are still scarce (Piovano et al., 2009) and are mainly focused on high-altitude playa complexes (i.e. Andean Altiplano and Puna; Fornari et al., 2001; Pueyo et al., 2001; Godfrey et al., 2003; Valero-Garcés et al., 2003).

The location of Salina de Ambargasta in central Argentina (28° 42′ to 29° 45′ S and 63° 57′ to 64° 38′ W; Fig. 1) combined with the availability of both hydrological and meteorological data, makes this saline complex a very attractive site to study sedimentological features in a low altitude playa system. Today, regional rainfall averages 600 mm/year, while evapotranspiration is approximately 1300 mm/year. Seasonal variations in addition to recent inter-decadal fluctuations in the precipitation–evaporation (P–E) ratio in central Argentina (Pasquini et al., 2006) have ruled the dynamics of this playa setting. The purpose of this paper is, therefore, to identify and characterise the modern depositional setting of Salina de Ambargasta, blending geomorphological, sedimentological and mineralogical results with cartography, satellite images and instrumental datasets. These results provide an analogue to further investigate the saline sedimentary record of Ambargasta. A characterisation of the modern setting is thus critical to reconstruct the Quaternary environmental evolution of this playa system that is located in a key area for palaeoenvironmental reconstructions.

2. Materials and methods

A field inspection of geomorphological features previously recognised in satellite images, aerial photographs and maps provided the basis for the identification of subenvironments. A Digital Elevation Model (DEM, Fig. 1) was generated based on topographical data available for the study area using Arc/GIS tools (Instituto Geográfico Militar de Argentina – IGM, http://srtm.usgs.gov, http://www.maproom.psu.edu/dcw).

Surface clastic sediment samples (SA-1–SA-9) as well as evaporite samples (Ev-1–Ev-5) were taken across different subenvironments (see sampling locations in Fig. 2). Granulometric fractions <500 μm were determined in surface sediments by a Cilas 1180 Laser Particle Size Analyzer at the Departamento de Ciencias Geológicas, Universidad de Buenos Aires (Argentina). Samples were previously dried in an oven at 60 °C and sieved through a 500 μm plastic sieve. Granulometric parameters were determined using the equations proposed by Folk (1968).

The mineralogy of clastic sediments and salt crusts was analysed by X-ray diffraction (XRD; SCINTAG XRD, 2000 Diffractometer) at the Université de Neuchâtel (Switzerland) and at the Universidad Nacional de Córdoba (Argentina). Sample preparation followed Kübler (1983) and the identification of whole rock composition was based on methods described by Ferrero (1966), Klug and Alexander (1974), and Kübler (1983). Mineralogical determinations also included scanning electron microscopy (SEM) coupled with an energy-dispersive X-ray (EDAX) analyser at the Section des Sciences de la Terre et de l'environnement, Université de Genève (Switzerland). Additional observations included smear-slides and thin sections. Techniques of smear slide preparation are described in http://Irc.geo.umn.edu/smears/smsl.htm.

Ultra high-resolution elemental analyses of spring precipitates were performed using micro X-ray fluorescence (Micro XRF) EAGLE III equipment. Samples were inspected under atmospheric conditions

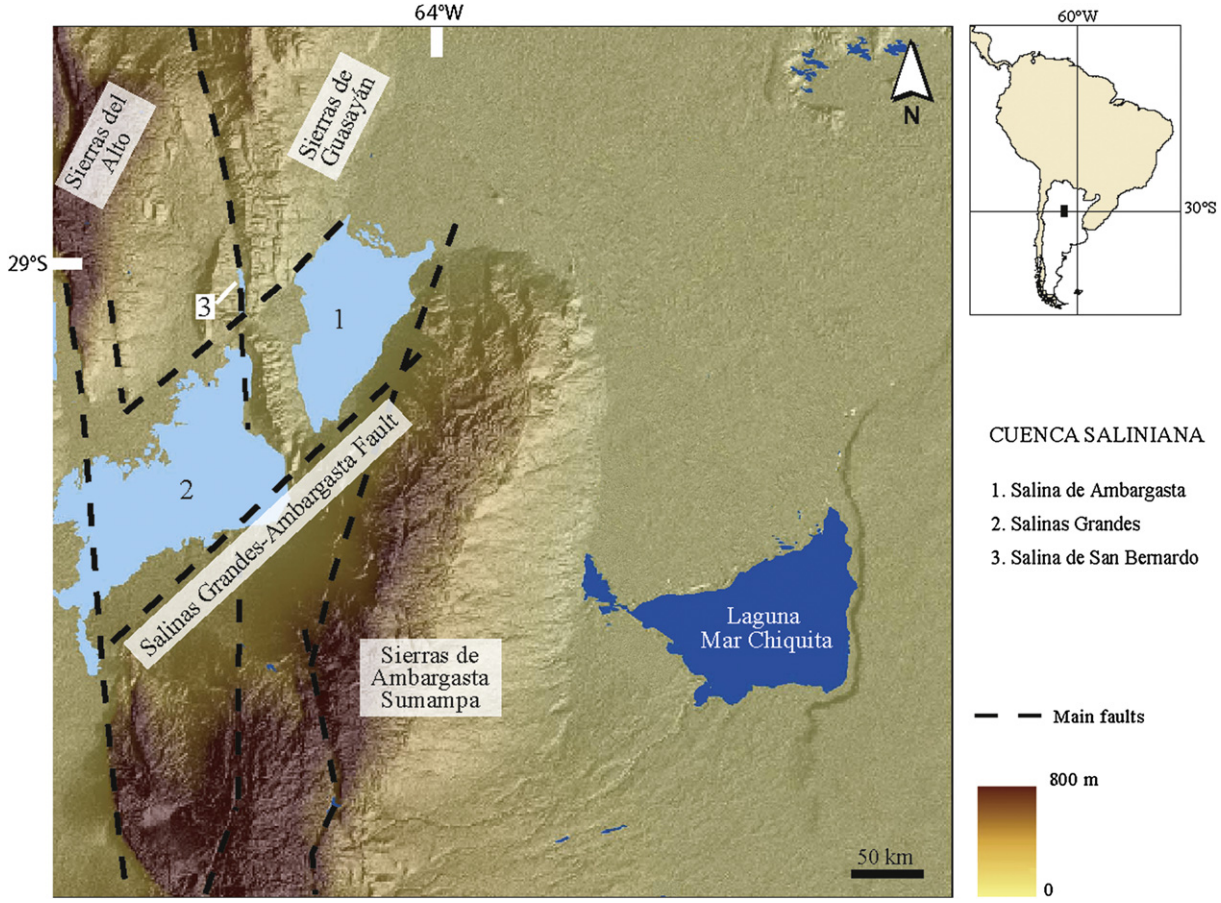

Fig. 1. Location of Salina de Ambargasta in South America. Digital elevation model of Cuenca Saliniana (saline systems are indicated by numbers) surrounded by Sierras Pampeanas. Salina La Antigua, also forming part of the Cuenca Saliniana, is located 38 km to the west of salinas Grandes (2). The location of Laguna Mar Chiquita is also indicated.

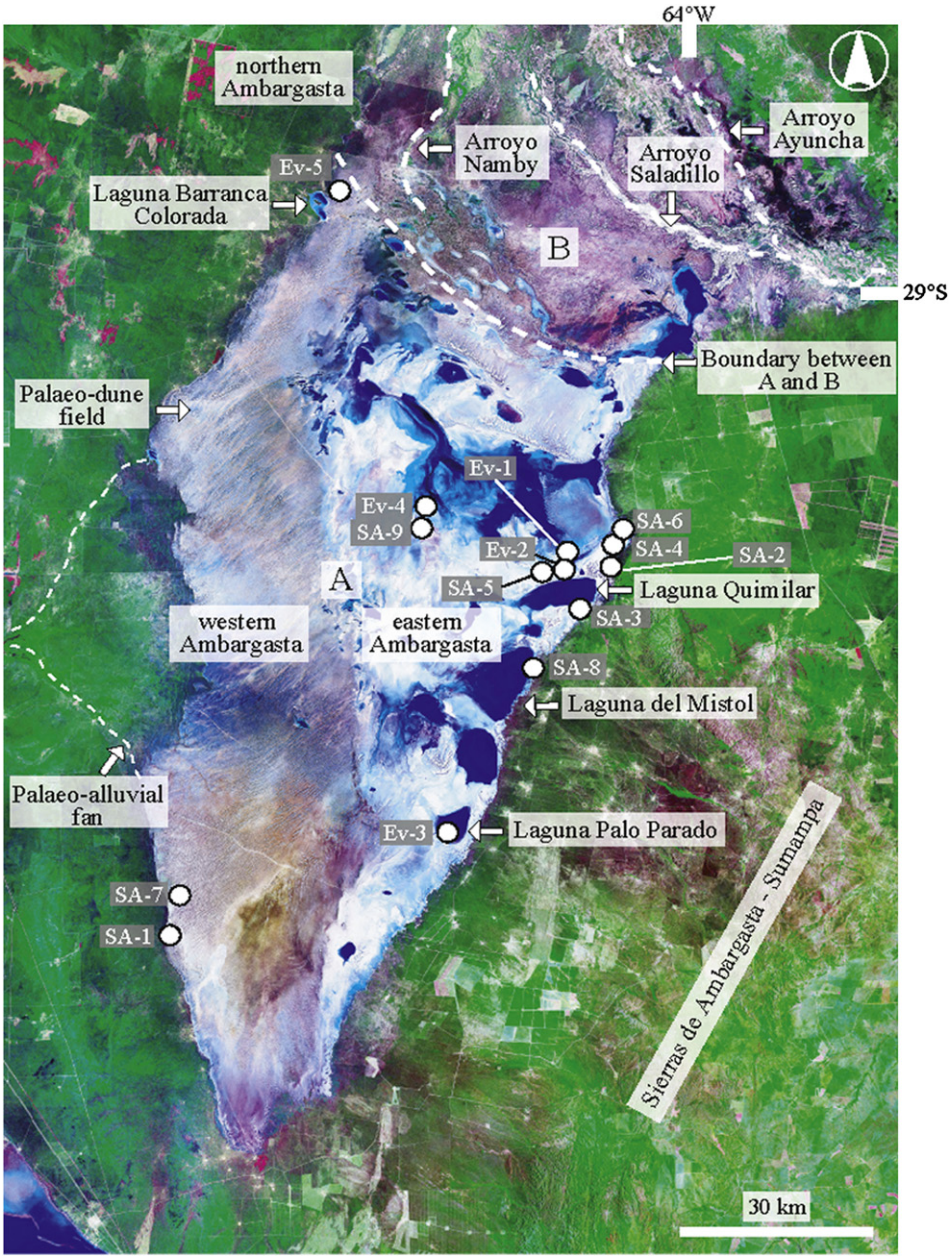

Fig. 2. Satellite image of the study area showing the location of sediment sampling points for granulometric and mineralogical determinations. The image also shows the two contrasting areas in Salina de Ambargasta: (A) closed system and (B) open-like system drained by Arroyo Saladillo. The boundary between A and B is indicated by a white dashed line. The three zones located at different topographical levels correspond to western Ambargasta, eastern Ambargasta and northern Ambargasta.

with a 50 μm diameter beam at the Section des Sciences de la Terre et de l'environnement, Université de Genève (Switzerland).

In-situ measurements of water physicochemical parameters including pH, temperature, alkalinity, total dissolved solids (TDS) and conductivity were carried out in playa lakes, streams (Arroyo Saladillo) and groundwaters of surrounding areas. Major ion concentrations of water samples (Na^+, Ca^{2+}, Mg^{2+}, K^+, Cl^-, SO_4^{2-}) were determined in the Service Commun d'Analyse Chimique (SCAC) – CEREGE (Aix-en-Provence, France). Cation concentrations (Ca^{2+}, Mg^{2+}, Na^+, K^+) were measured using 10 HNO_3 standards by Ultima-C Jobin Yvon Horiba Inductively Coupled Plasma-Atomic Emission Spectrometry (ICP-AES); anions (Cl^-, SO_4^{2-}) were measured by a Water Capillary Ion Analyser (WCIA) on a Quanta 4000 Millipore machine.

Stable isotope analyses of surficial and underground waters ($\delta^{18}O$ and δ^2H) were performed at CEREGE using a dual inlet Delta Plus Mass Spectrometer, by measuring successively CO_2 and H_2 gas equilibrated with water samples. The analytical precision was 0.05‰ for $\delta^{18}O$ and 1‰ for δ^2H. Results were reported in the conventional delta notation relative to the Vienna Standard Mean Ocean Water (VSMOW), on a scale normalised to Standard Light Antarctic Precipitation (SLAP) values. The $\delta^{18}O$ and δ^2H values for all water samples were compared to the World Meteoric Water Line (WMWL; Craig, 1961).

Precipitation data provided by the Servicio Meteorológico Nacional and Subsecretaría de Recursos Hídricos (Argentina, http://www.smn.gov.ar/ and http://www.hidricosargentina.gov.ar/) were analysed at seven meteorological stations: Caminiaga, Villa María

del Río Seco, San Francisco del Chañar, Gutemberg, Villa Ojo de Agua, Km88 and Santiago del Estero (see general information in Table 1 and locations in Fig. 3B), including monthly average precipitation covering the last 19–100 years. The Río Dulce monthly mean discharge record (Station No 8; see Table 1) was obtained from the Subsecretaría de Recursos Hídricos (Argentina). The austral summer corresponds to the period between December and March, while the austral winter is from June to September.

3. General geological setting and climate

Salina de Ambargasta (4200 km^2), together with the Salinas Grandes (4700 km^2), San Bernardo (7.2 km^2) and La Antigua (410 km^2) assemble one of the largest saline complexes in the world (Fig. 1). The salinas are located in the broken foreland basin of Sierras Pampeanas (Jordan and Allmendinger, 1986), occupying a large tectonic depression, namely Cuenca Saliniana (Álvarez et al., 1990). The Cuenca Saliniana is surrounded by the Sierras de Ambargasta-Sumampa to the east and the Sierras de Guasayán and the Sierras del Alto to the northwest (Fig. 1). The surrounding lithology is mainly composed of Precambrian to Palaeozoic metamorphic rocks intruded by granites (Rapela et al., 1998). The stratigraphy of the area includes Eopalaeozoic, Cretaceous, Tertiary and Quaternary units predominantly represented by continental deposits. Particularly, the adjacent area of Salina de Ambargasta includes Quaternary successions represented by alluvial fans, fluvial floodplains, mudflats and aeolian facies as well as ephemeral saline lake sediments.

The tectonic setting of the region is characterised by both transverse and longitudinal faults (illustrated in Fig. 1), associated with the Mesozoic and Tertiary Andean Orogeny, respectively (Ramos et al., 2002). The regional relief contains altitudes ranging from 115 to 120 m a.s.l. in the saline plain to a maximum of 800 m a.s.l. in the ranges (see Fig. 1). Within the saline complex, the topographical gradient decreases from west to east with a mean elevation of 118 m a.s.l. for the western zone and a mean elevation of 115 m a.s.l. in the eastern zone. A regional geological map for the area can be downloaded from http://www.segemar.gov.ar/p_regcentro/inicio.htm.

Regional climate is mainly defined by one of the major atmospheric features driving seasonal climatic variability in the SESA, the South American Monsoon System (Zhou and Lau, 1998). A distinguishable feature that controls the rainfall distribution in central Argentina is a southward warm air flux named the South American Low Level Jet (SALLJ), which transports moisture from the tropics to southeastern South America (Labraga et al., 2000). As a result, austral summer precipitation maxima and drier winters characterise a large area (including Ambargasta), reaching the east of the Andes between 22 and 40°S (Doyle and Barros, 2002). SALLJ inter-annual variability plays a fundamental role in the regional climate and largely determines the hydrological balance of the studied region. Recent changes in the water budget resulted in long dry intervals throughout the first 75 years of the 20th century, whereas an increasing trend in precipitation, lake water levels and river discharges in central Argentina have been recorded since the mid 1970s (Boulanger et al., 2005; Pasquini et al., 2006; Piovano et al., 2009; Troin et al., 2010).

Regional rainfall in Salina de Ambargasta ranges from 500 to 600 mm/yr and the total annual evapotranspiration can reach 1300 mm/yr (i.e., Villa Ojo de Agua Station, see Tables 1 and 2). The high insolation and evapotranspiration, as well as the prevalence of dry N, NNE and sometimes SW, NW–SE winds also contribute to a water deficit in the area (808 mm/year), as seen in Table 2. Annual precipitation data show that rainfall mainly occurs during the austral summer (Fig. 3A) with the annual precipitation increase produced by comparatively high summer rainfall (see also Table 2). Conversely, there is a negative trend during the dry season (austral winter) as a result of decreased winter rainfall. Winds blow mainly from September to December with an average velocity of 11.6 km/h (data from Servicio Meteorológico Nacional, Argentina).

4. Hydrology and hydrogeochemistry

Salina de Ambargasta is located in the Río Salí-Dulce catchment area, forming part of a major closed basin known as the Mar Chiquita system (Fig. 3B). The upper catchment of Río Salí-Dulce is situated in the Cumbres Calchaquies at 5500 m a.s.l., while the middle basin receives tributaries from low altitude areas (ca. 150 m a.s.l.), as shown in Fig. 3B. Before reaching the Laguna Mar Chiquita, the Río Dulce drains a very flat area forming marshy zones, ponds and a wetland in the northern part of the lake. Although Laguna Mar Chiquita (71 m a.s.l.) is the final destination of the Río Salí-Dulce catchment basin, Salina de Ambargasta represents another closed basin within the system that is, however, located at a comparatively higher topographical level (120 m a.s.l.). A lake water balance model investigating the link between climate, fluvial discharges and lake-level variations in the Mar Chiquita system can be found in Troin et al. (2010).

Regarding its hydrological behaviour, the playa complex can be subdivided into (Fig. 2): a) a closed system "*sensu-stricto*", where the loss of water is dominated by evaporation, and b) an "open-like system" located in the northernmost portion of the playa complex, where the Arroyo Saladillo acts as the seasonal outlet of numerous small lakes that may become linked during the wet season. The playa receives a significant amount of groundwater, but occasionally it can be fed by episodic and short-lived ephemeral streams. Groundwater flow is controlled by major linear tectonic structures and the water table is usually less than 2 m below ground level. Three main directions of surface flow prevail: NW–SE, SW–NE and E–W, while the density of channels is comparatively high in the northernmost portion of the playa (e.g. Arroyos Ayuncha and Namby in Fig. 2).

Table 1
Name, location, elevation, variable and record period of meteorological stations. The location of the stations (numbers) can be found in Fig. 3B.

No	Station	Latitude (S)	Longitude (W)	Elevation (m a.s.l.)	Variable	Period
1	Caminiaga	30° 04′	64° 03′	710	Rainfall	1941–1993
2	Villa Maria del Río Seco	29°54′	63° 41′	341	Rainfall	1957–2003
3	San Francisco del Chañar	29° 47′	63° 57′	700	Rainfall	1949–1994
4	Gutemberg	29° 44′	63° 32′	430	Rainfall	1940–1990
5	Villa Ojo de Agua	29° 31′	63° 42′	480	Rainfall	1986–2005
6	Km88	29° 17′	64° 08′	180	Rainfall	1977–2005
7	Santiago del Estero	27° 46′	64° 18′	200	Rainfall	1903–2003
8	Río Dulce	27° 35′	64° 30′	250	Discharge	1925–1980

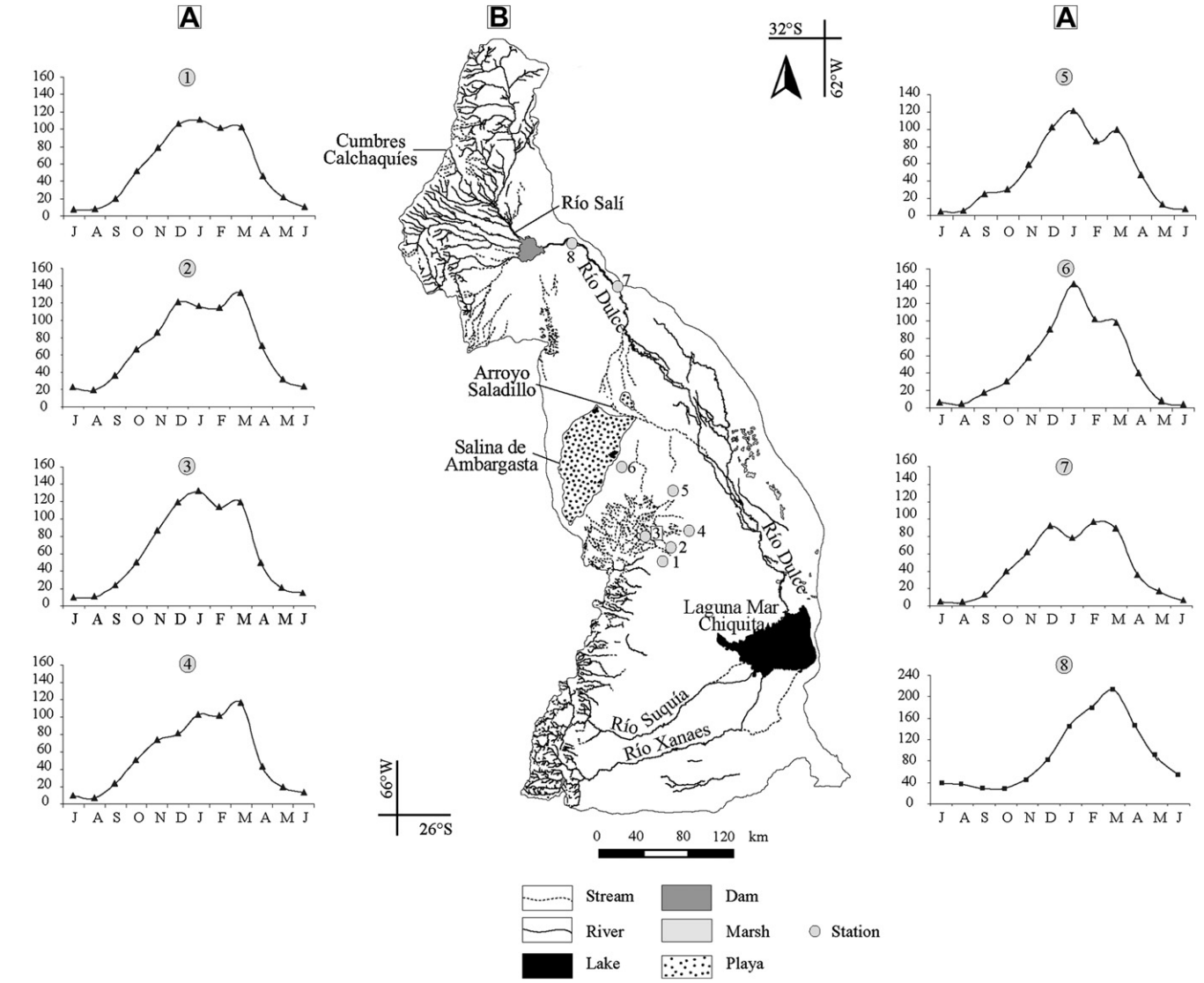

Fig. 3. (A) Monthly average precipitation (N° 1–N° 7) and discharge curve (N° 8) obtained from instrumental data at meteorological and discharge stations. The name of the stations can be found in Table 1. (B) Laguna Mar Chiquita endorheic basin showing the locations of Salina de Ambargasta, rivers, streams and lakes from the catchment area, and the analysed stations.

A negative hydrological balance (Table 2), in addition to the scarcity of channels, suggest that the playa lakes are mainly fed by groundwater input, whereas direct precipitation and runoff play a secondary role. Furthermore, the importance of groundwater contribution with respect to runoff is highlighted by the existence of springs and their associated chemical deposits (silcrete-calcrete duricrust) as well as by a high number of in-chain lakes following structural lineaments (see Fig. 2).

Major ion groundwater composition, shown in Table 3, presents a definite spatial trend (Fig. 4A and B). A compositional evolution

Table 2
Instrumental data (average values for the period 1986–2005) for Villa Ojo de Agua station (the location of the station is shown in Fig. 3B).

Month	Temperature (°C)	Precipitation (mm)	Evapotranspiration (mm)	Water balance (mm)
January	25.3	100	159	−59
February	25.1	58	137	−79
March	24.2	73	137	−64
April	18.1	45	100	−56
May	9.5	11	62	−51
June	11	2	64	−62
July	10.9	7	67	−60
August	13	7	80	−73
September	16.3	22	98	−76
October	20	36	127	−91
November	23	56	141	−86
December	25.1	108	160	−51
Annual	18.46	526	1334	−808

Table 3
Chemical parameters and major ionic concentrations (mg/L) of ephemeral saline lakes (Laguna Quimilar and Laguna Barranca Colorada), groundwaters and ephemeral stream (Arroyo Saladillo). Sampling locations are shown in Fig. 4A.

	Ephemeral saline lakes						Groundwater				Ephemeral stream
	Laguna Quimilar			Laguna Barranca Colorada							Arroyo Saladillo
Sample (N°)	1	2	3	4	5	6	8	9	10	13	14
Sampling dates	Feb-04	Apr-07	May-05	Feb-04	May-05	Nov-05	Aug-04	Jul-06	Nov-05	–	Nov-05
Depth (m)	0.15	0.15	0.15	0.15	0.15	0.15	18	69	4	21	surface
Temperature (°C)	33.5	32.9	15.3	36.5	23.4	35.1	n.d.	n.d.	25	n.d.	36.2
TDS (g/L)	33.5	n.d.	60.9	55.5	51.2	33.4	n.d.	n.d.	n.d.	n.d.	n.d.
Conductivity (ms/cm)	67.7	53.1	120.4	111.5	103.3	n.d.	n.d.	n.d.	n.d.	n.d.	n.d.
pH	8.58	8.57	8.08	7.87	8.95	9.8	7.8	7.9	7.8	6.6	10.37
Na^+	n.d.	n.d.	26,672	n.d.	22,740	14,571	345	70	962	311	4278
Ca^{2+}	n.d.	n.d.	1358	n.d.	575	801	12	12	19.6	b.d.l.	45
Mg^{2+}	n.d.	n.d.	73.4	n.d.	609	296	83	152	85.8	191	222
K^+	n.d.	n.d.	214	n.d.	234	193	15	26	16.8	17	12
HCO_3^-	n.d.	n.d.	n.d.	n.d.	n.d.	n.d.	249	205	n.d.	267	n.d.
CO_3^{2-}	n.d.	n.d.	n.d.	n.d.	n.d.	n.d.	0	540	n.d.	0	n.d.
Cl^-	n.d.	n.d.	36,478	n.d.	27,857	21,764	278	240	1110	450	15,264
SO_4^{2-}	n.d.	n.d.	5932	n.d.	11,005	9376	398	119	543	349	1660
Alkalinity	3025	53	4974[a]	3750	3235[a]	12,317	249[a]	205[a]	691	267[a]	12,867

n.d. not determined.
b.d.l. bellow detection limit.
[a] alkalinity calculated by AQUACHEM PHREEQC software.

occurs from the distal areas (Sierras de Ambargasta; see Fig. 2) downward to the sandflat in the margins of the saline playa, where groundwaters change from calcium magnesium-type (sample 13; Fig. 4A and B) to sodium-type (sample 10). In addition, as shown in Fig. 4A and B, chloride concentrations in groundwater samples increase towards the sandflat subenvironment.

Conversely, sodium chloride-type chemistry dominates the brine composition of the saline lakes of Ambargasta (Fig. 4B). Chloride concentrations in lake waters range from 21,764–36,478 mg/L, while maximum and minimum values of sodium are 26,672 and 14,572 mg/L, respectively (samples 3, 5 and 6; Fig. 4A and B). Higher values for both sodium and chloride correspond to

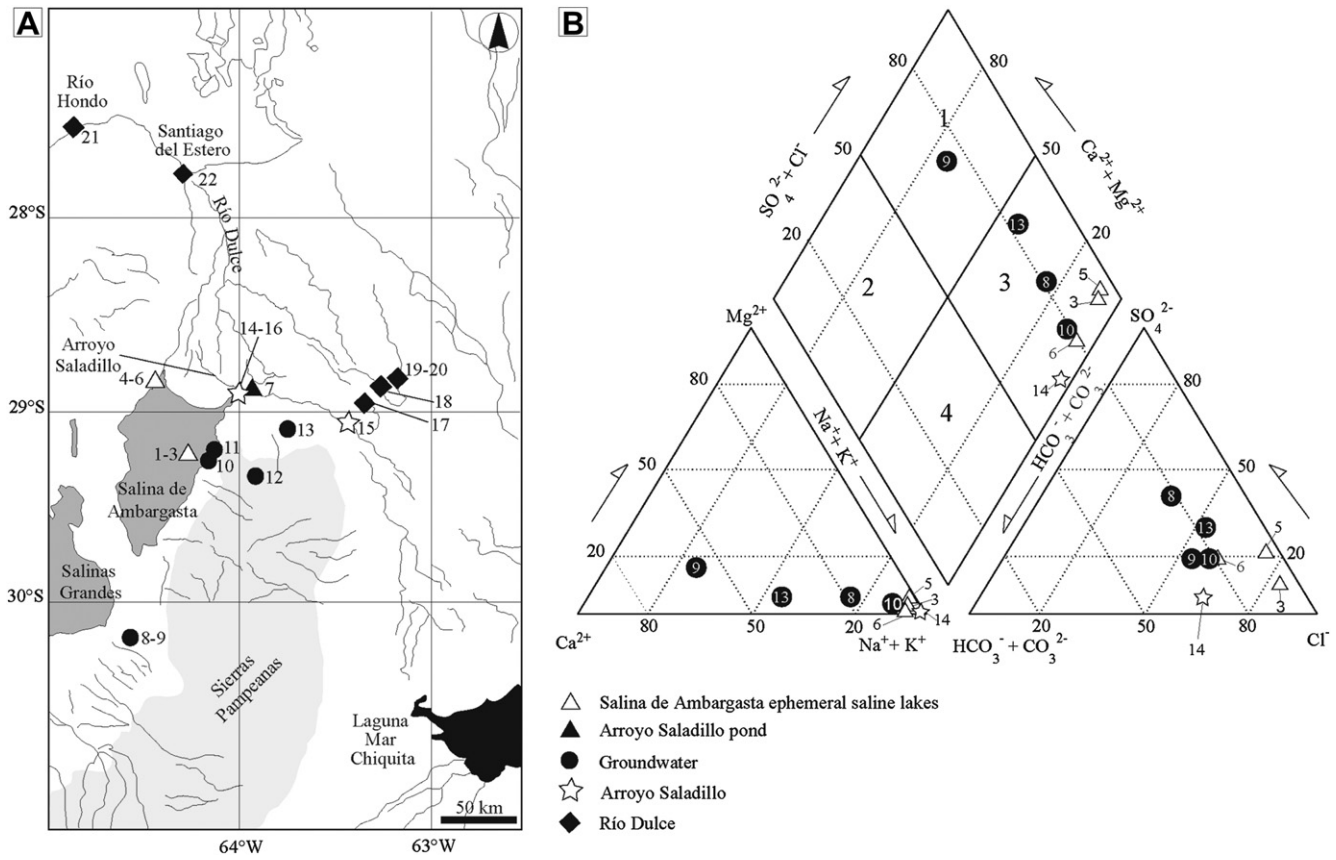

Fig. 4. (A) Map of the study area showing the locations of water samples for major ionic and isotopic concentrations (ephemeral saline lakes, Arroyo Saladillo pond, groundwater, Arroyo Saladillo and Río Dulce). The numbers of the samples are shown in Tables 3 and 4. (B) Chemical facies of the water samples analysed in the study area as defined in a Piper diagram (chemical data in Table 3).

Laguna Quimilar water samples (sample 3; Fig. 4B). Sulphate concentrations in lake waters range from 5932 to 11,005 mg/L and are higher in the Laguna Barranca Colorada (samples 5 and 6; Table 3 and Fig. 4A and B). Finally, the Arroyo Saladillo sample (sample 14, Table 3 and Fig. 4A and B), taken at the outlet of the playa complex, shows an intermediate ionic composition between the saline lakes and groundwater concentrations.

The chemical composition of lake waters is the result of chemical fractionation due to evaporation plus the dissolution of pre-existent evaporite deposits. Dargám (1995) observed in the neighbouring Salinas Grandes (see playa location in Fig. 4A), that the hydrochemistry of the zone between the source areas and the sandflat is governed by chemical weathering, whereas in the saline complex itself, the chemical composition is controlled by evaporation, fractional crystallization and salt dissolution. In consequence, the chemistry of sampled aquifers adjacent to the Ambargasta complex (samples 10 and 13; see Fig. 4A and B) represent the initial composition of brines in the playa system (samples 3, 5 and 6). Similarly, the more concentrated end-members in Salinas Grandes (Dargám, 1995) could be the result of evaporation of the distinctive groundwater-types in the distal areas (samples 8 and 9; Fig. 4A and B).

The stable isotope geochemistry ($\delta^{18}O$ and $\delta^{2}H$) from groundwater, rivers and lake water samples show a wide range of isotope ratios (Table 4 and Fig. 5). Groundwater samples (samples 10, 11 and 12; see sampling sites in Fig. 4A) show the lightest compositions in both $\delta^{18}O$ and $\delta^{2}H$, ranging from −5.20 to −6.70‰ (mean = −5.83‰) and −33.70 to −35.40‰ (mean = −34.73‰), respectively. All groundwater samples are located very close to the WMWL (especially samples 10 and 11; see Fig. 5), undoubtedly indicating that they did not undergo evaporation. One of the three groundwater samples (sample 12; Fig. 5) lies left of the WMWL, representing a more isotope-diluted water type, and probably represents local precipitation values for the Sierra de Ambargasta.

Río Dulce water samples (samples 17–22; Fig. 5) are also clustered very close to the WMWL showing more positive isotope ratios relative to groundwater samples, with an average $\delta^{18}O$ and $\delta^{2}H$ composition of −4.15 and −16.83‰, respectively (Table 4).

$\delta^{18}O$ values for Arroyo Saladillo (samples 14–16; Table 4) vary between −5.00 and 2.00‰ (mean = −2.43‰), while $\delta^{2}H$ compositions range from −32.70 to 14.60‰ (mean = −16.13‰). The $\delta^{18}O$ and $\delta^{2}H$ positive values correspond to a late spring water sample (sample 14, November 2005; see Table 4) suggesting that evaporation could be responsible for the isotopic enrichment of these waters.

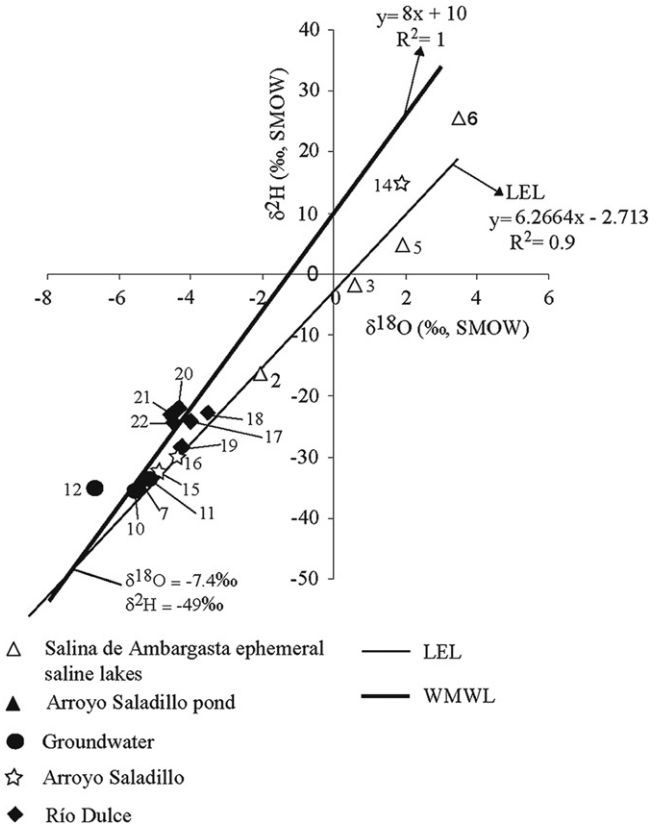

Fig. 5. $\delta^{18}O$ vs. $\delta^{2}H$ (‰) for ephemeral saline lakes, ponds, groundwater and rivers in the study area. The $\delta^{18}O$ and $\delta^{2}H$ values for all water samples are compared to the world meteoric water line (WMWL). Ambargasta isotopic data define a local evaporation line (LEL in the figure). The intersection of the WMWL and the local evaporation line (LEL) is expected to correspond to the composition of water that feeds the playa complex of Ambargasta ($\delta^{18}O$ = −7.4‰ and $\delta^{2}H$ = −49‰).

Table 4
Isotopic compositions ($\delta^{18}O$ and $\delta^{2}H$, ‰) of ephemeral saline lakes, ponds, groundwater, ephemeral stream (Arroyo Saladillo) and rivers (Río Dulce) from the catchment area. Sampling locations are shown in Fig. 4A.

Sample (N°)	Sampling Dates	$\delta^{18}O$ (‰)	$\delta^{2}H$ (‰)
Ephemeral saline lakes			
2	Apr-07	−2.10	−16.40
3	May-05	0.56	−2.40
5	May-05	1.89	4.20
6	Nov-05	3.45	25.33
Arroyo Saladillo pond			
7	Apr-07	−5.50	−34.70
Groundwater			
10	Nov-05	−5.60	−35.40
11	Apr-07	−5.20	−33.70
12	Apr-07	−6.70	−35.10
Arroyo Saladillo			
14	Nov-05	2.00	14.60
15	Apr-07	−5.00	−32.70
16	Apr-07	−4.30	−30.30
Rio Dulce			
17	Apr-07	−4.00	−24.00
18	Apr-07	−3.50	−23.10
19	Apr-07	−4.20	−28.70
20	Apr-07	−4.30	22.10
21	Apr-07	−4.50	−23.20
22	Apr-07	−4.40	−24.10

$\delta^{18}O$ and $\delta^{2}H$ values for the Arroyo Saladillo pond (sample 7; Table 4) are very similar to those of the groundwater samples (−34.70 and −5.50‰, respectively; Figs. 4A and 5), probably indicating that groundwater is the main source feeding this permanent pond.

Samples taken from saline lakes show the highest variability in isotopic compositions, accounting for the heaviest values in summer water samples (samples 2–6; Table 4 and Fig. 5). $\delta^{18}O$ compositions range from −2.10 to 3.45‰, while $\delta^{2}H$ values show an extremely large range from −16.40 to 25.33‰. All water lake samples from the Ambargasta saline system are isotopically enriched and lie under the WMWL (Fig. 5), indicating that evaporation is one of the most important mechanisms controlling the water isotopic composition in these environments.

Additionally, there is a clear seasonal trend towards increased $\delta^{18}O$ and $\delta^{2}H$ values, from sample 2 (April, austral autumn) to sample 6 (November, austral summer; Table 4 and Fig. 5), reflecting that lacustrine settings are very sensitive to changes in the precipitation/evaporation ratio throughout the year. Ambargasta isotopic data noticeably define a Local Evaporation Line (LEL, described by $y = 6.2664\times - 2.713$; $R^2 = 0.9$), as shown in Fig. 5. The intersection of the LEL and WMWL is expected to correspond to the composition of water that feeds the playa complex of Ambargasta. Groundwater (samples 10 and 11) and permanent pond (sample 7) isotopic compositions plot very close to this intersection, indicating that they represent the recharge water of the playa system.

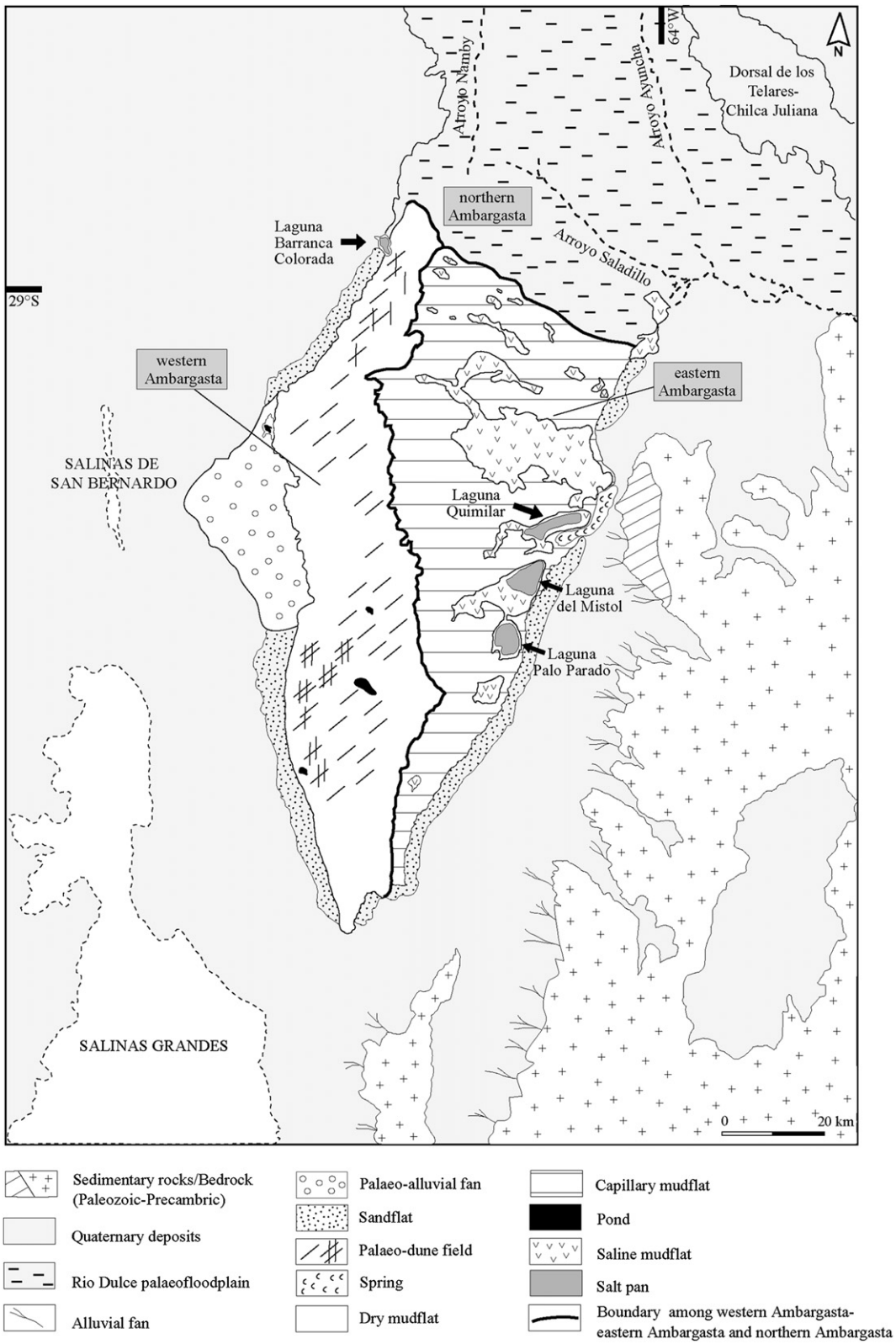

Fig. 6. Distribution of the sedimentary subenvironments in Salina de Ambargasta. The solid black lines indicate the boundary among western Ambargasta, eastern Ambargasta and northern Ambargasta. Dorsal de los Telares-Chilca Juliana is a topographical high that splits Río Dulce and Arroyo Saladillo.

5. Depositional subenvironments in Salina de Ambargasta

Geomorphological and sedimentological features enable identification of three well-defined zones located at different topographical levels, as shown in Fig. 2: western Ambargasta (mean elevation = 118 m a.s.l.), eastern Ambargasta (mean elevation = 115 m a.s.l.) and northern Ambargasta (mean elevation = 109 m a.s.l.). Along these three zones, the following depositional settings were

recognised (Fig. 6): (1) alluvial fan; (2) sandflat; (3) springs; (4) dunes and palaeo-dune field; (5) dry mudflat; (6) capillary mudflat; and (7) ephemeral saline lake (includes saline mudflat and salt pan).

The western zone is characterised by a dominant dry mudflat, small pluvial ponds and an eroded palaeo-dune field (Fig. 6). Conversely, the eastern area is comparatively more influenced by groundwater upflow triggering the formation of well-developed ephemeral saline lakes. The northern zone includes a wide floodplain of ca. 40 km length and 50 km width, which corresponds to the "open-like system" illustrated in Fig. 2 (see also Arroyo Saladillo in Fig. 7A and B).

5.1. Alluvial fan, sandflat, dunes and palaeo-dune field

Distal alluvial fans are mostly developed in the eastern area where they grade from the Sierra de Ambargasta-Sumampa into the sandflat (Fig. 6). These coalescing concave-shaped wedges, colonized by vegetation, gradually evolve towards fluvio-aeolian silts and sands. The mean slopes vary between 1.75% for the proximal fan and 0.75% for the distal fan (Angueira, 2003). The west-central margin of the salina is also reached by a mega-distal palaeo-alluvial fan of unknown age that is covered by halophyte vegetation (see Fig. 2).

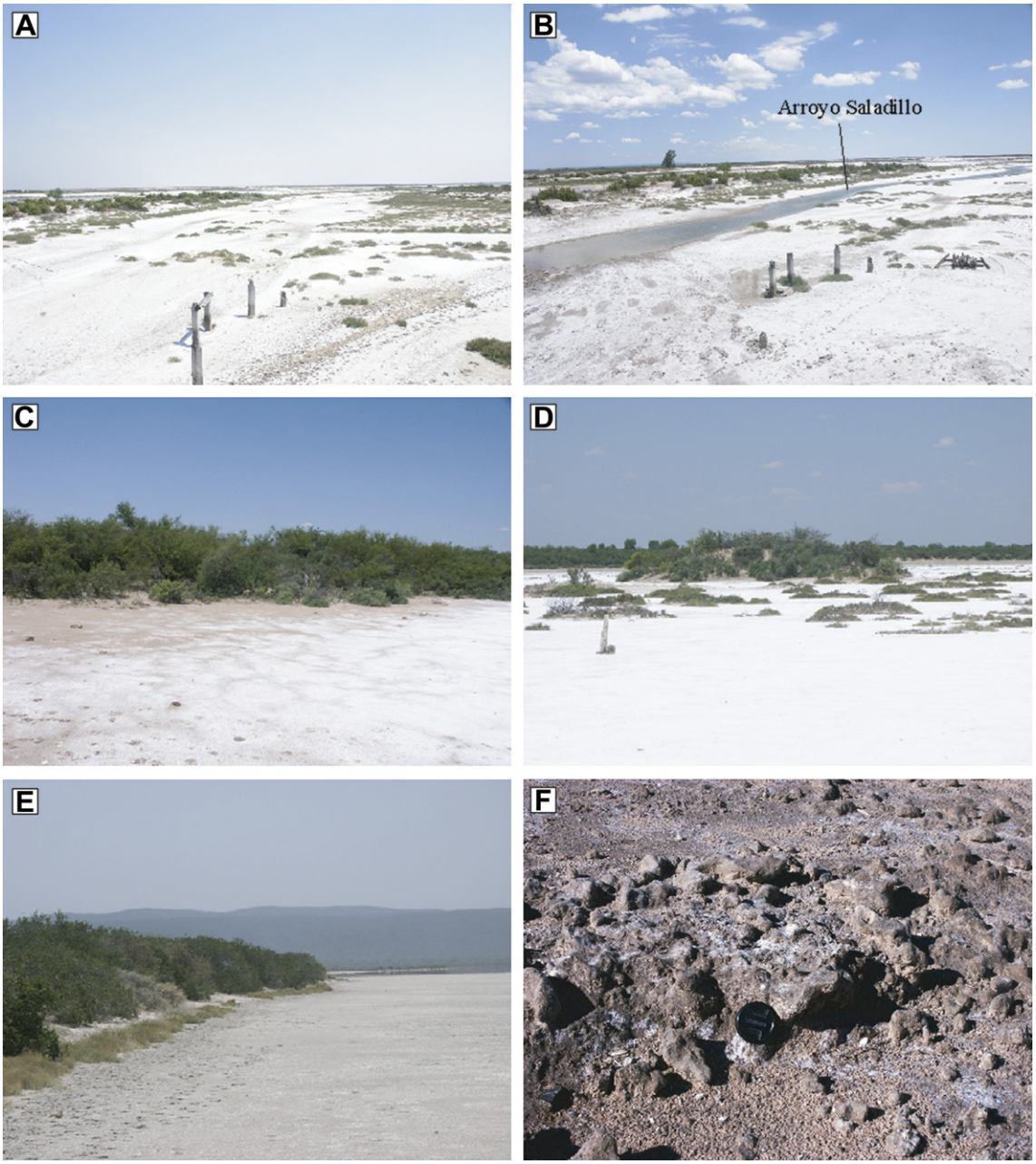

Fig. 7. Photographs of the different subenvironments in Salina de Ambargasta. (A) Dry channel and floodplain of Arroyo Saladillo. The photograph was taken in late summer when precipitation decreases and evapotranspiration remains high. Note the abundance of salt efflorescence and the presence of halophyte vegetation. (B) Arroyo Saladillo outflowing from northern Ambargasta during austral summer. The channel is 0.4 m deep. (C) Sandflat subenvironment of approximately 5 km width at the margin of the salina. (D) Groups of dunes of different sizes at the border of the salina. The largest dune is approximately 2 m high and is totally colonized by halophyte vegetation. (E) Elongated dune with predominant E–W direction stretching along the border of Laguna Quimilar. (F) Spring precipitates (silcrete-calcrete duricrust) in the eastern area (lense cap diameter is 5 cm).

Table 5
Granulometric parameters (mean particle size and sorting) calculated in surface sediment samples from sedimentary subenvironments. Sampling locations are shown in Fig. 2.

Sample	Subenvironment	Mean particle size (Mz)	Sorting (σ)
SA-1	Sandflat	3.49	1.49
SA-2	Sandflat	3.80	1.67
SA-3	Dune	2.93	1.40
SA-5	Dune	2.49	0.79
SA-7	Dry mudflat	5.31	2.05
SA-8	Capillary mudflat	5.52	1.99
SA-9	Capillary mudflat	6.11	1.77

Reddish sandflats rim the eastern and western margins of the playa covering an area between 5 and 10 km in width (Fig. 7C). Sediments in these aprons comprise poorly sorted very-fine sands (mean = 3.49 and 3.80 phi; samples SA-1 and SA-2, see sample locations in Fig. 2; Table 5). Sediments are massive or include planar-parallel horizontal lamination and/or ripple cross-laminated beds. The mineralogical composition is quartz, K-feldspar, albite, augite, hornblende, ilmenite, gypsum and anhydrite (sample SA-1; Table 6), suggesting the Sierras Pampeanas as the dominant source area. In this subenvironment, sediments are accumulated by wind action and additionally reworked by surficial runoff. These sandy aprons are completely occupied by halophyte plant species (e.g., *Aspidosperma* sp., *Cercidium australe, Prosopis chilensis*), as illustrated in Fig. 7C.

A palaeo-dune field in the western area consistss of two sets of superimposed dunes with N–S and NE–SW orientations (see Figs. 2 and 6). Dune junctions prevail in both NW and SW zones; however, single members with a NE–SW direction dominate in almost all of the western area. The dune system has been reworked by ephemeral runoff and exhibits crest lowering. It is also colonized by vegetation indicating a non-migratory behaviour of the system. Eroded dunes range from 40 to 50 cm in height, can be up to tens of m wide and between 3 and 7 km long. This palaeo-dune field could represent a relict feature formed during earlier periods of the Quaternary. Similar sand dune systems are observed in different zones in western Argentina (34–36°S and 66–68°W; Tripaldi and Forman, 2007), reflecting multiple dune reactivations during dry events since the Late Quaternary.

Sand dunes, isolated or forming groups, are common features located around the margins of the salina (Fig. 7D). They are completely stabilized by vegetation and comprise a wide range of sizes, between 0.20 and 2 m in height and up to 2 m in length. Sediments in this subenvironment are generally poorly sorted (sample SA-3; see sample locations in Fig. 2; Table 5) with a mean particle size of very-fine sand to fine sand (Mz = 2.93 phi). Mineralogical examinations reveal that quartz, K-feldspar, andesine, albite, augite, biotite, gypsum and anhydrite are the major components found in this subenvironment (sample SA-4; Table 6).

Other types of vegetated sand dunes stretch along the border of a few saline lakes forming elongated structures with predominant E–W direction (Fig. 7E). A sediment sample taken from a large dune parallel to the margin of Laguna Quimilar (sample SA-5; see sample locations in Fig. 2) is a moderately sorted fine sand (Mz = 2.49 phi; Table 5). Elongated sandy dune stabilization could be promoted by groundwater contribution through subsurface fracture systems. Wetter conditions in these structures allow extensive growth of vegetation which trap and gradually accumulate clastic sediments, transported by both wind and surface runoff.

5.2. Springs

Springs are located in the central-eastern portion at the intersection between sandflats and mudflats, producing small ponds and precipitates (Figs. 7F and 8). Associated duricrusts are hard, brown continuous layers of approximately 0.5 m in thickness showing nodular morphology and compositional banding (Fig. 8A). Bulk sample mineralogical analyses indicate that quartz, K-feldspar, andesine, hornblende, biotite, ilmenite and calcite are the principal mineral components (sample SA-6; Table 6). A high proportion of volcanic glass is inferred from X-ray diffractograms. Compositional changes can be identified through thin section (Fig. 8B–D) and Micro XRF examinations. There is an upper portion, named phase I, (Fig. 8A and B) that is composed of a brownish clay matrix mainly cemented by micrite calcite including extraclasts (quartz, K-feldspar, Ca-plagioclase, biotite, chlorite; see Fig. 8C). Phase II, at lower portions (Fig. 9A and B), is composed of fine, cryptocrystalline silica cement (Fig. 8D), embedding white/grey clastic sheets of coarser mineral fragments and abundant volcanic glass. Micro XRF analyses along the duricrust (A–D transect in Fig. 8A) show that phase I is enriched in Ca, while phase II displays higher Si contents (Fig. 8E). Si shows the opposite behaviour related to Ca across both phases. These results reveal that the spring precipitates correspond to a mixed-type grading from silica to carbonate cement. Nash and Shaw (1998) proposed the term silcrete-calcrete intergrade duricrust to describe these types of precipitates that are formed under fluctuating groundwater conditions.

Table 6
XRD bulk mineralogy of surface sediment samples from different subenvironments. Sampling locations (SA-1–SA-9 and EV-1–Ev-5) can be found in Fig. 2. Dashes indicate no detection.

Sample	SA-1		SA-4		SA-6	SA-7	SA-8	Ev-1	Ev-2	Ev-3	Ev-4	Ev-5
Subenvironment	Sandflat		Dune		Spring Cal-silcrete duricrust	Dry Mudflat	Capillary Mudflat	Salt pan	Salt pan	Salt pan	Salt pan	Salt pan
	>30 μm	>30 μm	>30 μm	<30 μm								
Quartz	*	*	*	*	*	*	*	–	–	–	–	–
K-feldspar	*	*	*	*	*	*	*	–	–	–	–	–
Plagioclase (andesine)	–	–	*	*	*	*	*	–	–	–	–	–
Plagioclase(albite)	*	*	*	*	–	–	–	–	–	–	–	–
Augite	–	*	*	–	–	*	–	–	–	–	–	–
Hornblende	*	–	–	–	*	–	–	–	–	–	–	–
Biotite	–	–	*	*	*	*	–	–	–	–	–	–
Ilmenite	*	–	–	–	*	–	–	–	–	–	–	–
Calcite	–	–	–	–	*	–	*	–	–	–	–	–
Gypsum	*	–	–	*	–	–	*	* (2%)	* (3%)	* (3%)	* (2%)	* (3%)
Anhydrite	*	*	–	*	–	–	–	–	–	–	–	–
Halite	–	–	–	–	–	*	*	* (98%)	* (97%)	* (97%)	* (98%)	* (97%)

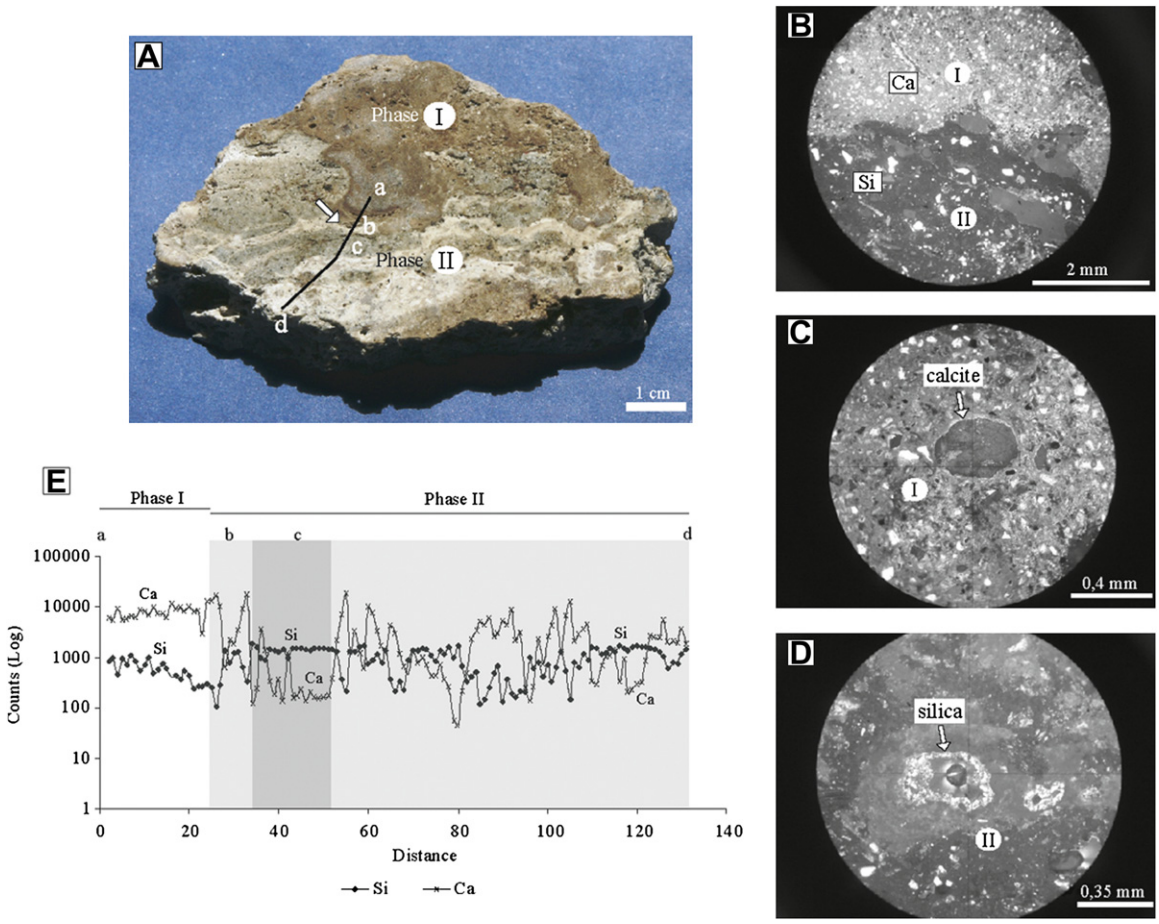

Fig. 8. Silcrete-calcrete duricrust in the eastern margin of the playa. (A) Photograph of the duricrust showing phases I (mainly carbonate) and II (mainly silica) and the A-B-C-D transect analysed by micro XRF. (B–D). Thin section photomicrographs. (B) Plane polarized light, boundary between the carbonatic (phase I) and silica (phase II) cement. (C) Plane polarized light, sparry calcite cement around a quartz intraclast. (D) Crossed polars, inward growing of silica in a pore within phase II. (E) Relative abundance of Si and Ca determined by micro XRF.

5.3. Dry mudflat

Dry mudflat is restricted to the western area (Fig. 6). This setting is characterised by the presence of a vegetal cover *(Allenrolfea sp.; Suaeda sp.*; Fig. 9A) and the general scarcity of water bodies. The development of small intermittent ponds (ca. 20 m^2 and 15 cm deep; Fig. 9B) is restricted to the SW border, whilst only one ephemeral saline lake can be identified in the NW portion (see Laguna Barranca Colorada in Fig. 2).

Sediments in the dry mudflat are composed mostly of poorly sorted, reddish-brown fine silts (Mz = 5.3 phi; sample SA-7, see sample location in Fig. 2; Table 5). XRD bulk mineralogical analyses show that sediments are primarily composed of quartz, K-feldspar, andesine, augite, biotite and halite (sample SA-7; Table 6). Sediments are capped by an efflorescent salt crust (up to 0.5 cm thick), precipitated from subsurface brines drawn up to the surface by evaporative pumping (Hsü and Siegenthaler, 1969; Last, 1984; 1989). The efflorescence, composed of halite, are drier, powdery and thinner when compared to efflorescence developed in the capillary and saline mudflats. Similar situations were described by Smoot and Castens-Seidell (1994) in Saline Valley and Death Valley (California). As noted by Yechieli and Wood (2002), aeolian process dynamics depend on the depth of the groundwater level. Because in this setting the aquifer is situated at a greater depth (approximately 1.5 m) relative to the neighbouring mudflats, materials at the surface remain dry (especially during austral autumns and winters) and can potentially be removed by deflation.

Ponds are formed during the rainy season leading to the development of microbial mats almost completely covering the pond floor. Below the microbial communities, there is a black anaerobic layer of decomposed organic matter, which is approximately 5 cm thick, as seen in Fig. 9C. A few cm-scale mudcracks develop during winter desiccation, indicating a short-lived existence.

5.4. Capillary mudflat

A capillary mudflat is located in the eastern sector, occupying the area between the dry mudflat and the saline mudflat (Fig. 6). This subenvironment is classified as a different mudflat type, as it has intermediate features between the two mudflats mentioned above. It is defined by the total absence of vegetation (Fig. 9D), the presence of intermittent ponds and the lack of interstitial saline minerals. Similar descriptions have also been reported in other saline systems by Last and Schweyen (1983), Last (1984), and Sonnenfeld and Perthuisot (1989). The groundwater table, unlike the dry mudflat, stands closer to the surface (approximately 1 m), allowing the development of thicker efflorescent salt crusts (up to 1 cm thick). The efflorescence is composed almost exclusively of halite.

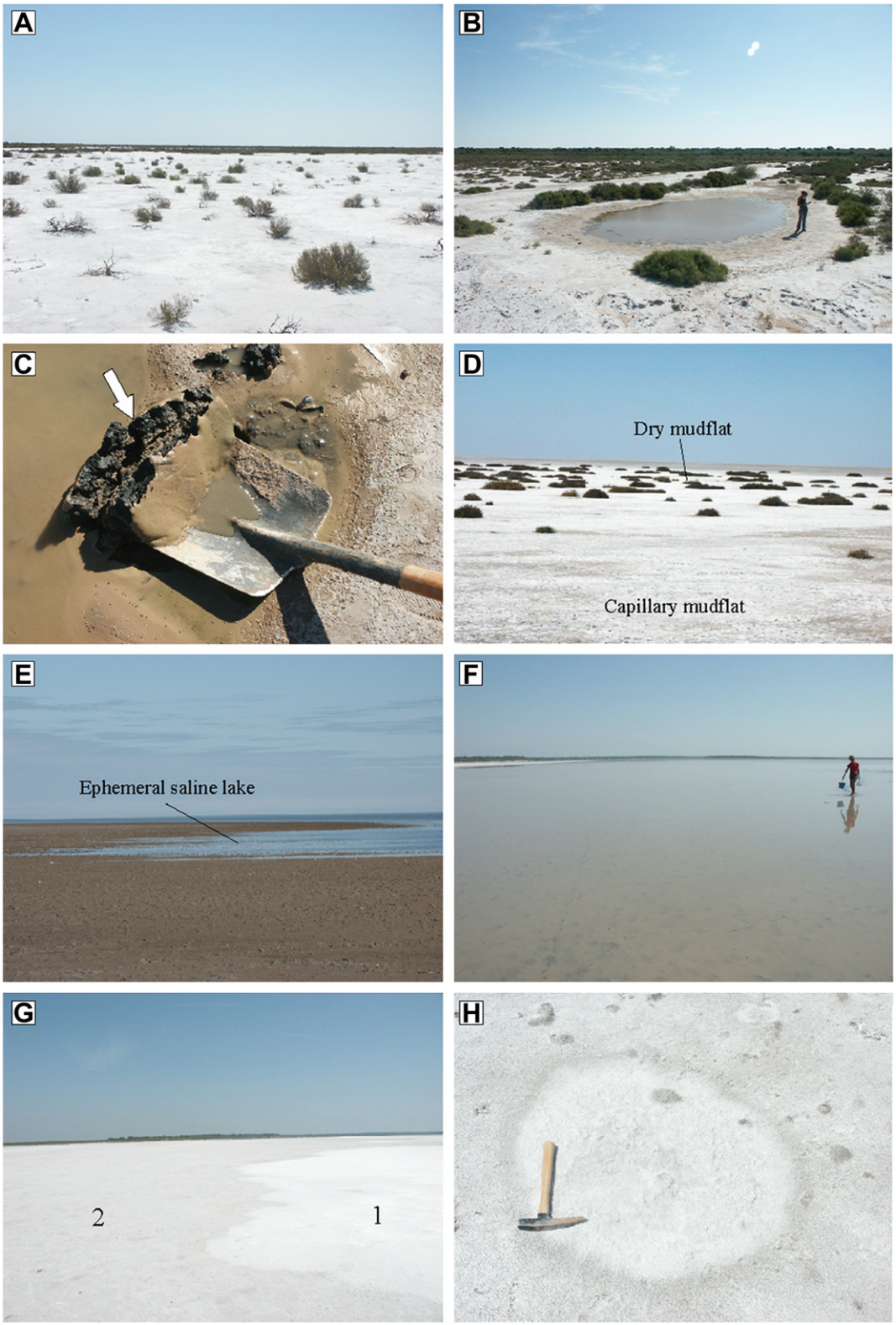

Fig. 9. Photographs of the different subenvironments at Salina de Ambargasta. (A) Dry mudflat characterised by the presence of halophyte vegetation and thin efflorescence. (B) Intermittent pond in the dry mudflat covering a surface area of about 20 m^2. (C) Black anaerobic layer (approximately 5 cm thick) of decomposed organic matter on the pond floor. (D) Dry and capillary mudflats. Note the absence of vegetation in the capillary mudflat. (E) Laguna Barranca Colorada ephemeral saline lake on the NW border of the salina. Water depth is about 15 cm. (F) Laguna Quimilar ephemeral saline lake in the eastern area of the salina. Water depth is about 30 cm (G) 1. Salt pan composed almost exclusively of halite (2 cm thick) fringed by a saline mudflat (2). (H) Crystal bowl of 1 m diameter developed in the deepest areas of the ephemeral saline lake subenvironment.

Surficial sediments comprise very poorly sorted, brownish fine silts (Mz = 5.52 and 6.11, samples SA-8 and SA-9 respectively, see sample locations in Fig. 2; Table 5). Bulk sample mineralogical analyses show that quartz is the most abundant phase, with subordinate amounts of K-feldspar and andesine (sample SA-8; Table 6). Evaporite minerals correspond to calcite, gypsum and halite.

5.5. Ephemeral saline lake (includes the saline mudflat and the salt pan)

Ephemeral saline lakes are mainly restricted to the eastern part of the Ambargasta saline complex (Figs. 2 and 6). The very low lake density in the western zone is noticeable, where only intermittent ponds and one ephemeral saline lake (Laguna Barranca Colorada; Fig. 9E) are present (see also Fig. 2).

Field observations during the years 2004–2009 indicate that most of the lakes in the eastern area correspond to the ephemeral-type, since they dry up once a year during the austral winter. However, water bodies may persist without drying up for a few years, as was observed in the late 1970s, when a wet phase took place in central Argentina (Piovano et al., 2004). The descriptions of Hardie et al. (1978), Pueyo (1979) and Hudec and Sonnenfeld (1989) were followed to classify this setting.

The largest ephemeral saline lakes are Laguna Quimilar (Fig. 9F), Laguna Mistol, Laguna Palo Parado and Laguna Barranca Colorada (see their locations in Fig. 2). The first three lakes are located at the lowermost central-east zone and the latter at the NW portion (Fig. 6). The mean lake area ranges from 35 to 45 km^2 during summer, while it is reduced to 10–20 km^2 during winter. The lakes normally reach a maximum water depth of 20 cm. Additionally, these temporary lakes can migrate following the dominant wind direction (NW) and this leads to the development of lakes with an asymmetrical morphology (see Fig. 2).

Fluctuations in the hydrological balance throughout the year trigger the flooding and desiccation stages of the lakes. After the lakes are flooded by meteoric waters, they begin shrinking by the intense evaporation during the late summer. Whenever the lakes completely dry up, as in the case of Laguna Quimilar, Laguna Mistol, Laguna Palo Parado and Laguna Barranca Colorada, a salt pan forms in the lowest part of the lake area (Fig. 9G). The salt pan is a crystalline salt layer of variable thickness, as outlined by Hardie et al. (1978). In the Ambargasta lakes, the salt pans typically reach no more than 2.5 cm in thickness and are composed almost exclusively of cubic halite and minor quantities of gypsum (samples Ev-1–Ev-5: 97–98% and 2–3%, respectively; Table 6). Frequently, instead of forming an extensive continuous salt pan in the lowest portions of the lake, it develops small crystal bowls of a diameter of 1 m, separated from each other by muddy sediments (Fig. 9H). Lakes with these special features were termed “spotted lakes” by Renaut and Long (1989). The expansion and contraction cycles of the lakes and their sedimentation are explained in the following section.

Immediately fringing the salt pans, a muddy zone is left exposed when the saline lakes are diminished in size, remaining soaked with subsurface brine. This area composed of clastic sediment crowded with salt crystals precipitated by evaporative pumping, is named the “saline mudflat” by Hardie et al. (1978), and Smoot and Lowenstein (1991). In the Salina de Ambargasta, the sediments of the saline mudflat are similar to the capillary mudflat and consist of reddish, massive silty clays; however, intrasedimentary growth of halite is restricted to the saline mudflat. The sediments are almost permanently saturated with brines (unlike the capillary mudflat) due to the influence of the water table located very close to the surface. The surface of this setting is covered by a white, 1-2 cm thick efflorescent crust of halite (see Fig. 9G). There is a total absence of vegetation in the saline mudflat. Similar deposits in the saline mudflat/salt pan subenvironment were analysed by Smoot (1983) in the Wilkins Peak Member of the Green River Formation (U.S.A.).

6. Playa lake dynamics

According to the annual hydrological balance, playa lakes exhibit expansion, shrinking and finally, a complete desiccation (Lowenstein and Hardie, 1985, Fig. 10A–C). Transgressive phases occur during the rainy season when lakes are fed by groundwater inflow, surface runoff and direct precipitation (Fig. 10A). Precipitation, evapotranspiration and temperatures attain their maximum values during the summer months (see values in Table 2). Meteorological data also show that average evapotranspiration was

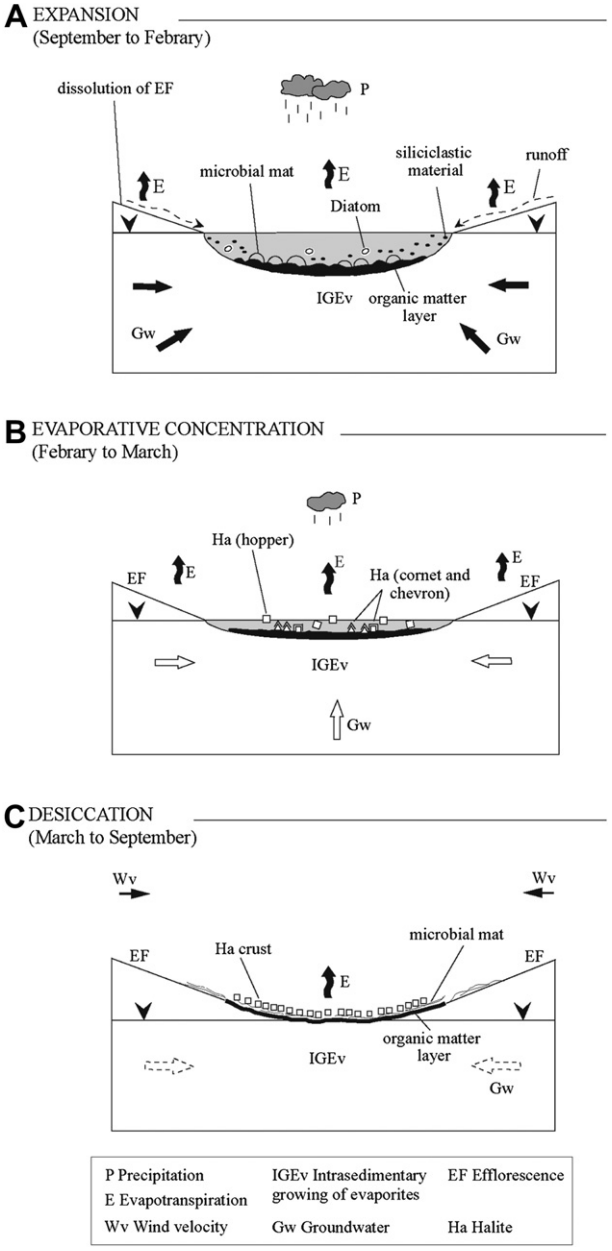

Fig. 10. Schematic model representing ephemeral saline lake dynamics in Salina de Ambargasta. (A) Expansion stage during austral summer. (B) Evaporative concentration in late summer and (C) Desiccation phase during drier months. Higher groundwater inflows are indicated by black arrows, whereas white and dashed arrows indicate comparatively low inputs. Note that runoff is exclusive of the flooding stage.

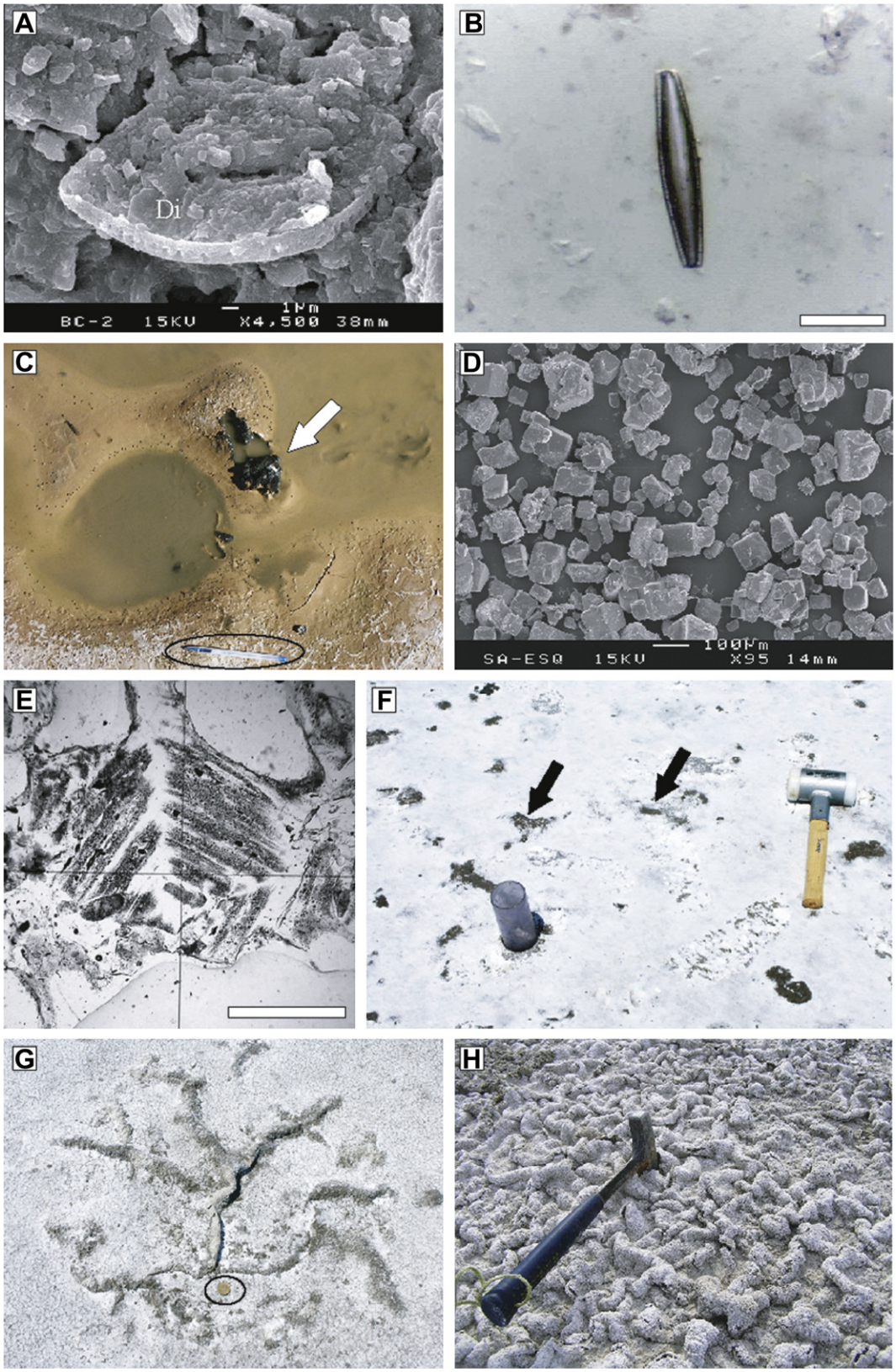

Fig. 11. Photographs illustrating the different phases of ephemeral saline lake dynamics. (A) Expansion phase, SEM photomicrograph of diatom (Di) embedded in a clay matrix. (B) Expansion phase, smear slide photomicrograph of diatom. Scale bar: 0.1 mm. (C) Expansion phase, elliptic dome structures produced by the occlusion of gases below the microbial mats (pen for scale). White arrow shows a collapsed dome. (D) Evaporative concentration, cumulates of cubic halite crystals directly precipitated from lake water. (E) Evaporative concentration, thin section of halite crystal with hopper texture precipitated at the brine surface. Scale bar: 0.1 mm. (F) Desiccation phase, salt crust previously precipitated from lake water covering the dome structures formed during the lake expansion phase. Black arrows show the exposed dome. (G) Desiccation phase, wrinkled morphologies produced by contraction of the microbial mats (coin for scale). (H) Desiccation phase, contorted structures produced by putrefaction of the microbial mats.

persistently higher than precipitation. This interval, with higher runoff and groundwater inflows, is recorded by the deposition of fine-grained siliciclastic sediments forming a blanketing layer of mud at the lake bottom. Dissolution of the former halite-rich efflorescent crusts by floodwaters, in addition to a high evapotranspiration during this period, produces a dominant chloride-type brine in the playa (see chemical data in Table 3). This freshening state is accompanied by relatively high biological activity. SEM and smear slide observations show different species of diatom remains within the massive clay (Fig. 11A and B). Flooding is also accompanied by the extensive growth of microbial mats covering the entire lake floor. Below the microbial mats, a black sapropelic layer develops, reaching no more than 5 cm thick, formed by decomposed organic matter. A strong fetid smell in these sediments suggests the reduction of sulphates by the action of sulphate-reducing bacteria (Teller et al., 1982; Valero-Garcés et al., 1999; 2000). Interesting features observed on the lake floor are elliptic dome structures up to 30 cm in diameter (Fig. 11C). Similar dome-shaped structures were described by Pueyo (1979) in the saline lakes of Zaragoza and Teruel (Spain). Below the microbial mats the occlusion of gases (probably methane) is considered to produce these ellipsoidal domes. The gas bubbles are probably generated by decay of the underlying sapropelic layer, as reported by Hardie et al. (1978).

The following evaporative concentration stage starts during the late summer when precipitation decreases considerably, evapotranspiration remains high and the lakes are principally fed by groundwater supply (Fig. 10B). The progressive brine concentration leads to direct precipitation of halite from lake water (Fig. 11D). When the brine reaches the halite saturation point, crystallization starts at the brine-air interphase as hopper (Fig. 11E) and raft textures. With time, crystals sink to the lake floor where syntaxial overgrowth may take place resulting in chevrons and cornet halite. These processes are very well described by Hardie et al. (1983), Lowenstein and Hardie (1985), Shubel and Lowenstein (1997) and Benison and Goldstein (2000), among others. The duration of the evaporative concentration phase is mostly governed by the hydrological balance of the preceding summer (i.e. longer phases occur after more humid summers). Analogous illustrations of ephemeral saline lake/salt pan cycles are presented in Renaut and Gierlowski-Kordesch (2010).

At the end of the summer, the standing waters of the expanded lakes begin shrinking by a persistent high evapotranspiration, and finally they dry up starting the lake desiccation stage (Fig. 10C). No rainfall is generally recorded from June to September – sometimes until November during dry years – leading to a desiccation phase that persists until the next rainy period. The final product of the lake contraction is the development of a 2 cm thick salt pan, mostly composed of cubic halite and an associated saline mudflat at the salt pan margins (see Fig. 9G). After the playa lake dries out, the salt crust previously precipitated from the lake water covers the numerous dome structures formed during the lake expansion phase (Fig. 11F). However, the salt crust gradually disappears by deflation and occasional runoff, and is replaced by the development of salt efflorescence precipitated from subsurface brines by evaporative pumping. During this stage, it is common that the deformation of the microbial mats as the result of contraction due to the complete desiccation of the lake surfaces produce a variety of wrinkled morphologies (Fig. 11G). In other cases, the putrefaction of the microbial communities leads to the development of contorted structures, as shown in Fig. 11H. Wind velocities are the strongest during this phase contributing to the desiccation of the water masses. Vandervoort (1997) have described diverse desiccation-related features in evaporite deposits of northwest Argentina, related to saline lake-level fluctuations.

7. Conclusions

Regarding its hydrological behaviour, the saline complex of the Salina de Ambargasta can be separated into a closed system "*sensu-stricto*" and an "open-like system" where the Arroyo Saladillo acts as the outlet of numerous in-chain small lakes.

The high abundance of clastic sediments and the development of thin salt crusts indicate that the Ambargasta system represents the mud-rich end member in the range of playa settings mentioned by Handford (1981) that extends from soluble salt or carbonate-sulphate sediments to terrigenous clastic-dominated playas. This fact limits the potential of this playa for the economic exploitation of salt minerals. Conversely, the nearby Salinas Grandes receives a more important water inflow – both surface runoff and groundwater– and consequently, this playa complex holds larger saline lakes promoting the formation of thicker evaporite facies.

Geomorphological and sedimentological features allow separation of the saline complex into three zones located at different topographical levels. Along these three zones the following distinctive settings were identified: (1) alluvial fan; (2) sandflat; (3) springs; (4) dunes and palaeo-dune field; (5) dry mudflat; (6) capillary mudflat, and (7) ephemeral saline lake (includes saline mudflat and salt pan).

This multicomponent system shows major changes in the dynamics of the subenvironments that are ruled by inter-annual hydrological variability as well as seasonal variations in precipitation. Dry mudflats occupy the highest western portions of the playa where groundwater influence is less important and only intermittent lakes are associated with this setting. On the other hand, the eastern low areas include ephemeral saline lakes dominated by lake transgressive–regressive cycles. From the beginning of the rainy season (austral summer) lakes experience expansions followed by an evaporative concentration and pervasive desiccation phase during the dry season. During the transgressive phase, lakes are flooded both by runoff and by groundwater inflows and these more dilute waters trigger the development of microbial mats and abundant diatoms species. This expansion stage, characterised by a higher organic productivity, is recorded as a black organic matter layer with a strong fetid smell probably due to sulphate-reducing bacteria. During late summer a generalized lake regressive phase takes place and water bodies begin shrinking by evaporation. Increasing salinity further leads to cubic halite growth, mostly with hopper and raft textures. When the desiccation stage occurs, ephemeral saline lakes switch to a salt pan in the deepest zone of the lake and a saline mudflat in the supralittoral areas until the next rainy season. Sandflats occur along the playa perimeter and they are associated with distal alluvial fans.

The dominant type of water in the playa lakes is a sodium chloride-type brine which results from chemical fractionation and salt dissolution processes. The increase of sodium and chloride in ephemeral saline lakes with respect to magnesium and calcium is the result of progressive evaporation of the distinctive groundwater-types. On the other hand, the isotopic composition ($\delta^{18}O$ and $\delta^{2}H$) of the lake waters compared with groundwater and river samples from the catchment area show that lake brines account for the heaviest values suggesting evaporation is the main process controlling the isotopic signals. Furthermore, these data reveal an obvious seasonal trend towards increased $\delta^{18}O$ and $\delta^{2}H$ compositions from lake samples taken during the drier months to samples taken during the rainy season. This fact is in agreement with instrumental data which reflect that both precipitation and evapotranspiration are higher during the austral summer. Seasonal variations in the isotopic compositions from ephemeral saline lakes also highlight the sensitivity of these settings to changes in the hydrological budget throughout the year.

This characterization of the modern environments within the Salina de Ambargasta provides an analogue to reconstruct past hydrological changes for this region during the Quaternary. Ongoing studies of sedimentary cores (up to 10 m long) retrieved in key locations of Salina de Ambargasta will further provide new data about the temporal evolution of this system that can additionally be used to interpret similar deposits in the geological record.

Acknowledgements

Different aspects of the results presented here have been carried out at CIGES-CICTERRA (Universidad de Córdoba, Argentina), Section des Sciences de la Terre et de l'environnement and the Intitut F.-A. Forel (Université de Genève, Switzerland). We wish to acknowledge A. Pasquini for helping with instrumental data analyses. We gratefully thank R. Martini (Université de Genève) for her help with the SEM as well as Université de Neûchatel (Switzerland) for XRD analyses. Adiela Martinez is specially thanked for her invaluable help during the DEM preparation. We gratefully acknowledge the Service Commun d'Analyse Chimique (SCAC) – CEREGE (Aix-en-Provence, France) for water samples analyses. We wish to acknowledge the financial support of Argentina's CONICET (http://www.conicet.gov.ar/), through PIP 5947, SECYT-UNC 2010-2011 (http://www.secyt.unc.edu.ar) and FONCYT (http://www.agencia.secyt.gov.ar/foncyt.php) through PICT 25594, and Federal Commission for Scholarships for Foreign Students (DHA/OFES – Switzerland) for providing a scholarship to Gabriela Zanor. We are grateful to G. Simpson (Université de Genève) and Zsuzsa Hoffmann for correcting the English text.

References

Abbott, M.B., Wolfe, B.B., Wolfe, A.P., Seltzer, G.O., Aravena, R., Mark, B.G., Polissar, P.J., Rodbell, D.T., Rowe, H.D., Vuille, M., 2003. Holocene paleohydrology and glacial history of the central Andes using multiproxy lake sediment studies. Palaeogeography, Palaeoclimatology, Palaeoecology 194, 123–138.

Allen, P.A., Collinson, J.D., 1986. Lakes. In: Reading, H.G. (Ed.), Sedimentary Environments: Processes, Facies and Stratigraphy, third ed. Blackwell Science, Oxford, pp. 63–94.

Álvarez, L.A., Fernández Seveso, F., Pérez, M.A., Bolatti, N.D., 1990. Estratigrafía de la Cuenca Saliniana. XI Congreso Geológico Argentino, San Juan. Actas 2, 145–148.

Angueira, C., 2003. Sistema de Información Geográfico de Santiago del Estero. SigSE 1.0. Available on line at:. INTA – ProSusNOA http://sigse.inta.gov.ar/acerca.htm.

Benison, K.C., Goldstein, R.H., 2000. Sedimentology of ancient saline pans: an example from the Permian Opeche Shale, Williston basin, North Dakota, U.S.A. Journal of Sedimentary Research 70 (1), 159–169.

Bobst, A.L., Lowenstein, T.K., Jordan, T., Godfrey, E.L., Ku, V.T., Luo, S., 2001. A 106 ka paleoclimate record from drill core of the Salar de Atacama, northern Chile. Palaeogeography, Palaeoclimatology, Palaeoecology 173, 21–42.

Boulanger, J.P., Leloup, J., Penalba, O., Rusticucci, M., Lafon, F., Vargas, W., 2005. Observed precipitation in the Paraná-Plata hydrological basin: long-term trends, extreme conditions and ENSO teleconnections. Climate Dynamics 24, 393–413.

Brodtkorb, A., 1999. Salinas Grande y Chica de la península de Valdés, Chubut. In: Zappettini, E. (Ed.), Recursos Minerales de la R. Argentina, 35. Instituto de Geología y Recursos Minerales, SEGEMAR (Buenos Aires), Anales, pp. 1971–1976.

Cohen, A.S., 2003. Paleolimnology: The History and Evolution of Lake Systems. Oxford University Press, New York, 500 p.

Craig, H., 1961. Isotopic variations in meteoric waters. Science 133, 1833–1834.

Dargám, R.M., 1994. Dinámica evolutiva y geoquímica de aguas y salmueras del ambiente evaporítico de las Salinas Grandes, Provincia de Córdoba, Argentina. Ph.D. thesis, Universidad Nacional de Córdoba.

Dargám, R.M., 1995. Geochemistry of waters and brines from the Salinas Grandes basin, Cordoba, Argentina. I. Geomorphology and hydrochemical characteristics. International Journal of Salt Lake Research 3, 137–158.

Doyle, M., Barros, V.R., 2002. Midsummer low-level circulation and precipitation in subtropical South America and related sea surface temperature anomalies in the South Atlantic. Journal of Climate 15, 3394–3410.

Eugster, H.P., Jones, B.F., 1979. Behavior of major solutes during closed-basin brine evolution. American Journal of Science 279, 609–631.

Ferrero, J., 1966. Nouvelle méthode empirique pour le dosage des minéraux par diffraction R.X. Rapport C.F.P. (Bordeaux), inédit.

Folk, R.L., 1968. Petrology of Sedimentary Rocks. Hemphill's, Austin, Texas. 170 p.

Fornari, M., Risacher, F., Féraud, G., 2001. Dating of paleolakes in central Altiplano of Bolivia. Palaeogeography, Palaeoclimatology, Palaeoecology 172, 269–282.

Fritz, S.C., Baker, P.A., Lowenstein, T.K., Seltzer, G.O., Rigsby, C.A., Dwyer, G.S., Tapia, P.M., Arnold, K.K., Ku, T.-L., Luo, S., 2004. Hydrologic variation during the last 170,000 years in the southern hemisphere tropics of South America. Quaternary Research 61, 95–104.

Godfrey, L.V., Jordan, T.E., Lowenstein, T.K., Alonso, R.L., 2003. Stable isotope constraints on the transport of water to the Andes between 22° and 26°S during the last glacial cycle. Palaeogeography, Palaeoclimatology, Palaeoecology 194, 299–317.

González, M.A., Maidana, N., 1998. Post-Wisconsinian paleoenvironments at Salinas del Bebedero basin, San Luis, Argentina. Journal of Paleolimnology 20, 353–368.

Grosjean, M., Cartajena, I., Geyh, M.A., Nuñez, L., 2003. From Proxy data to paleoclimate interpretation: the mid-Holocene paradox of the Atacama Desert, northern Chile. Palaeogeography, Palaeoclimatology, Palaeoecology 194, 247–258.

Handford, R.C., 1981. A process-sedimentary framework for characterizing recent and ancient sabkhas. Sedimentary Geology 30, 255–265.

Hardie, L.A., Eugster, H.P., 1970. The evolution of closed-basin brines. Mineralogical Society of America 3, 273–290.

Hardie, L.A., Smoot, J.P., Eugster, H.P., 1978. Saline lakes and their deposits: a sedimentological approach. In: Matter, A., Tucker, M. (Eds.), Modern and Ancient Lake Sediments, 2. IAS Spec, pp. 7–41.

Hardie, L.A., Lowenstein, T.K., Spencer, R.J., 1983. The problem of distinguishing between primary and secondary features in evaporites. Sixth International Symposium on Salt I, 11–39.

Hsü, J.K., Siegenthaler, C., 1969. Preliminary experiments on hydrodynamic movement induced by evaporation and their bearing on the dolomite problem. Sedimentology 12, 11–25.

Hudec, P.P., Sonnenfeld, P., 1989. Comparision of composition and concentration of some lagoonal and continental brine lakes. Sedimentary Geology 64, 265–270.

Jones, B.F., Deocampo, D.M., 2003. Geochemistry of saline lakes. In: Drever, J.I. (Ed.), Surface and Ground Water, Weathering and Soils. Treatise on Geochemistry, vol. 5(13). Elsevier, New York, pp. 393–424.

Jordan, T.E., Allmendinger, R.W., 1986. The Sierras Pampeanas of Argentina: a modern analogue of Rocky Mountain foreland deformation. American Journal of Science 286, 737–764.

Klug, H.P., Alexander, L., 1974. X-ray Diffraction Procedures for Polycrystalline and Amorphous Materials, First and second eds. John Wiley and Sons, New York.

Kübler, B., 1983. Dosage quantitatif des minéraux majeurs des roches sédimentaires par diffraction X. Cahier de l'Institut de Géologie de Neuchâtel. Série AX No 1.1 & 1.2.

Labraga, J., Frumento, O., López, M., 2000. The atmospheric water vapour cycle in South America and the tropospheric circulation. Journal of Climate 13, 1899–1915.

Last, W.M., Schweyen, T.H., 1983. Sedimentology and geochemistry of saline lake of the Great Plains. Hidrobiología 105, 245–263.

Last, W.M., 1984. Sedimentology of playa lakes of the northern Great Plains. Canadian Journal of Earth Sciences 21, 107–125.

Last, W.M., 1989. Continental brines and evaporites of the northern Great Plains of Canada. Sedimentary Geology 64, 207–221.

Last, W.M., Vance, R.E., 1997. Bedding characteristics of Holocene sediments from salt lakes of the northern Great Plains, Western Canada. Journal of Paleolimnology 17, 297–318.

Lowenstein, T.K., Hardie, L.A., 1985. Criteria for the recognition of salt-pan evaporites. Sedimentology 32, 627–644.

Lowenstein, T.K., Hein, M.C., Bobst, A.L., Jordan, T.E., Ku, T.-L., Luo, S., 2003. An assessment of stratigraphic completeness in climate-sensitive closed-basin lake sediments: Salar de Atacama, Chile. Journal of Sedimentary Research 73, 91–104.

Moreno, A., Giralt, S., Valero-Garcés, B., Sáez, A., Bao, R., Prego, R., Pueyo, J.J., González-Sampériz, P., Taberner, C., 2007. A 14 kyr record of the tropical Andes: the Lago Chungará sequence (18°S, northern Chilean Altiplano). Quaternary International 161, 4–21.

Nash, D.J., Shaw, P.A., 1998. Silica and carbonate relationships in silcrete-calcrete intergrade duricrusts from the Kalahari of Botswana and Namibia. Journal of African Earth Sciences 27, 11–25.

Pasquini, A.I., Lecomte, K.L., Piovano, E.L., Depetris, P.J., 2006. Recent rainfall and runoff variability in central Argentina. Quaternary International 158, 127–139.

Piovano, E., Ariztegui, D., Damatto Moreira, S., 2002. Recent environmental changes in Laguna Mar Chiquita (Central Argentina): a sedimentary model for a highly variable saline lake. Sedimentology 49, 1371–1384.

Piovano, E., Larizzatti, F.E., Fávaro, D.I.T., Oliveira, S.M.B., Damatto Moreira, S., Mazzilli, B.P., Ariztegui, D., 2004. Geochemical response of a closed-lake basin to 20th century recurring droughts/wet intervals in the subtropical Pampean Plains of South America. Journal of Limnology 63, 21–32.

Piovano, E.L., Ariztegui, D., Córdoba, F., Cioccale, M., Sylvestre, F., 2009. Hydrological variability in south America below the tropic of Capricorn (Pampas and eastern Patagonia, Argentina) during the last 13.0 ka. In: Vimeux, F., Sylvestre, F., Khodri, M. (Eds.), Past Climate Variability from the Last Glacial Maximum to the Holocene in South America and Surrounding Regions: From the Last Glacial Maximum to the Holocene, 14. Springer – Developments in Paleoenvironmental Research Series (DPER), pp. 323–351.

Pueyo, J.J., 1979. La precipitación evaporítica actual en las lagunas saladas del área: Bujaraloz, Vástago, Caspe, Alcañiz y Calanda (provincias de Zaragoza y Teruel). Revista del Instituto de Investigaciones Geológica 33, 5–56. Universidad de Barcelona.

Pueyo, J.J., Chong, G., Jensen, A., 2001. Neogene evaporates in desert volcanic environments: atacama Desert, northern Chile. Sedimentology 48, 1411–1431.

Ramos, V.A., Cristallini, E.O., Pérez, D.J., 2002. The Pampean flat-slab of the central Andes. Journal of South American Earth Sciences 15, 59–78.
Rapela, C.W., Pankhurst, R.J., Casquet, C., Baldo, E., Saavedra, J., Galindo, C., 1998. Early evolution of the Proto-Andean margin of south America. Geology 8, 707–710.
Renaut, R.W., Long, P.R., 1989. Sedimentology of the saline lakes of the Cariboo plateau, Interior British Columbia, Canada. Sedimentary Geology 64, 239–264.
Renaut, R.W., Gierlowski-Kordesch, E.H., 2010. Lakes. In: James, N., Dalrymple, R. (Eds.), Facies Models, fourth ed. Geological Association of Canada.
Richaser, F., Alonso, H., Salazar, C., 2003. The origin of brines and salts in Chilean salars: a hydrochemical review. Earth Science Reviews 63, 249–293.
Rosen, M.R., 1994. The importance of groundwater in playas: a review of playa classification and the sedimentology and hydrology of playas. In: Rosen, M.R. (Ed.), Paleoclimate and Basin Evolution of Playa Systems, 289. Geological Society of America Special Paper, pp. 1–18.
Schreiber, B.C., 1986. Arid Shorelines and evaporites. In: Reading, H.G. (Ed.), Sedimentary Environments and Facies, third ed. Blackwell Science, Oxford, pp. 189–228.
Shubel, K.A., Lowenstein, T.K., 1997. Criteria for the recognition of shallow-perennial-saline-lake halites based on recent sediments from the Quaidam Basin, western China. Journal of Sedimentary Research 67 (1), 74–87.
Smoot, J.P., 1983. Depositional subenvironments in an arid closed basin; the Wilkins Peak member of the Green River formation (Eocene), Wyoming, U.S.A. Sedimentology 30, 801–827.
Smoot, J.P., Lowenstein, T.K., 1991. Depositional environments of non-marine evaporates. In: Melvin, J.L. (Ed.), Evaporites, Petroleum and Mineral Resources. Elsevier, Amsterdam, pp. 189–347.
Smoot, J.P., Castens-Seidell, B., 1994. Sedimentary features by efflorescent salt crusts, saline Valley and Death Valley, California. In: Renaut, R.W., Last, W.M. (Eds.), Sedimentology and Geochemistry of Modern and Ancient Saline Lakes, 50. SEPM Spec. Publ, pp. 73–90.
Sonnenfeld, P., Perthuisot, J.P., 1989. Brines and evaporites. In: Crawford, M.A., Padovani, E. (Eds.), Short Course in Geology. American Geophysical Union, Washington DC.
Spencer, R.J., Eugster, H.P., Jones, B.F., Rettig, S.L., 1985. Geochemistry of Great salt Lake, Utah I: hydrochemistry since 1850. Geochimica et Cosmoschimica Acta 49, 727–737.
Sylvestre, F., Servant, M., Servant-Vildary, S., Causse, C., Fournier, M., Ybert, J.-P., 1999. Lake-Level chronology on the southern Bolivian Altiplano (18°–23°S) during late-glacial time and the early Holocene. Quaternary Research 51, 54–66.
Talbot, M.R., Allen, P.A., 1996. Lakes. In: Reading, H.G. (Ed.), Sedimentary Environments: Processes, Facies and Stratigraphy, third ed. Blackwell Science, Oxford, pp. 83–124.
Teller, J.T., Bowler, J.M., Macumber, P.G., 1982. Modern sedimentation and hydrology in Lake Tyrrell, Victoria. Journal of the Geological Society of Australia 29, 159–175.
Tripaldi, A., Forman, S.L., 2007. Geomorphology and chronology of Late Quaternary dune fields of western Argentina. Palaeogeography, Palaeoclimatology, Palaeoecology 251, 300–320.
Troin, M., Vallet-Coulomb, C., Sylvestre, F., Piovano, E., 2010. Hydrological modelling of a closed lake (Laguna Mar Chiquita, Argentina) in the context of 20th century climatic changes. Journal of Hydrology, 233–244.
Valero-Garcés, B.L., Delgado-Huertas, A., Ratto, N., Navas, A., 1999. Large ^{13}C enrichment in primary carbonates from Andean Altiplano lakes, northwest Argentina. Earth and Planetary Science Letters 171, 253–266.
Valero-Garcés, B.L., Delgado-Huertas, A., Navas, A., Machín, J., González-Sampériz, P., Kelts, K., 2000. Quaternary palaeohydrological evolution of a playa lake: Salada Mediana, central Ebro Basin, Spain. Sedimentology 47, 1135–1156.
Valero-Garcés, B.L., Delgado-Huertas, A., Navas, A., Edwards, L., Schwalb, A., Ratto, N., 2003. Patterns of regional hydrological variability in central southern Altiplano (18°–26°S) lakes during the last 500 years. Palaeogeography, Palaeoclimatology, Palaeoecology 194, 319–338.
Vandervoort, D.S., 1997. Stratigraphic response to saline lake-level fluctuations and the origin of cyclic nonmarine evaporite deposits: the Pleistocene Blanca Lila Formation, northwest Argentina. GSA Bulletin 109, 210–224.
Warren, J.K., 1999. Evaporites: Their Evolution and Economics, first ed.. Blackwell Science. 438 p.
Yan, J.P., Hinderer, M., Einsele, G., 2002. Geochemical evolution of closed-basin lakes: general model and application to Lakes Qinghai and Turkana. Sedimentary Geology 148, 105–122.
Yechieli, Y., Wood, W.W., 2002. Hydrogeologic processes in saline systems: playas, sabkhas and saline lakes. Earth Science Reviews 58, 343–365.
Zhou, J., Lau, K.M., 1998. Does a monsoon climate exist over South America? Journal of Climate 11, 1020–1040.